Winter 1-31-2023

Azimuthal Anisotropy of Different Quark-flavored Particles in High Energy "simulated" Proton-Proton Collisions

Mahmoud Rateb
rateb@aucegypt.edu

The American University in Cairo

الجامعة الأمريكية بالقاهرة

Graduate Studies

Azimuthal Anisotropy of Different Quark-flavored Particles in High Energy "simulated" Proton-Proton Collisions

A THESIS SUBMITTED BY

MAHMOUD RATEB

TO THE

Physics
Graduate Program

September 8, 2022

in partial fulfillment of the requirements for the degree of
Master of Science in Physics

Declaration of Authorship

I, Mahmoud Rateb, declare that this thesis titled, “Azimuthal Anisotropy of Different Quark-flavored Particles in High Energy "simulated" Proton-Proton Collisions” and the work presented in it are my own. I confirm that:

- This work was done wholly or mainly while in candidature for a research degree at this University.
- Where any part of this thesis has previously been submitted for a degree or any other qualification at this University or any other institution, this has been clearly stated.
- Where I have consulted the published work of others, this is always clearly attributed.
- Where I have quoted from the work of others, the source is always given. With the exception of such quotations, this thesis is entirely my own work.
- I have acknowledged all main sources of help.
- Where the thesis is based on work done by myself jointly with others, I have made clear exactly what was done by others and what I have contributed myself.

Signed:

_____

Date:

_____

Abstract

Anisotropic flow in high energy heavy-ion collisions is taken as a key evidence for the formation of QGP for brief seconds right after the collisions. Hydrodynamic models including QGP formation are accurate at predicting the azimuthal anisotropy of the produced particles at low transverse momenta. At high momenta however, hydrodynamic models predict no azimuthal anisotropy for particles of different masses and quark-flavors; the logic being that because of their high momenta, the particles pass through the media without having any time to have any reactivity. This is contrary to results from experiments where measurements of particles of different quark flavors show non-zero elliptic flow.

To study this deviation, we run PYTHIA simulation of proton-proton collisions at center-of-mass energies equivalent to those at RHIC and LHC; 200 GeV and 13 TeV. Since in PYTHIA simulations no QGP if formed, and there is no final-state interaction, results in our simulation would act as probes to be compared to the results of elliptic flow from real experiments.

Our results showed non-zero results for the elliptic flow of pions, heavy mesons and direct photons. Those results are evident of the possible bias in the way the reaction plane is calculated, since all the other factors are controlled for in the PYTHIA simulations. To make up for this inherent bias, the results from PYTHIA should be subtracted from the results of elliptic flow in real experiments, to end up with unbiased results for elliptic flow from the different colliders.

Acknowledgments

I would like to express my sincere gratitude to my advisor Dr. Ahmed M. Hamed for his patience, motivation, and immense knowledge. His guidance helped me in all the time of research and writing of this thesis.

In addition, I would like to thank my family and friends for supporting me spiritually throughout writing this thesis and in my life in general.

Contents

List of Figures

List of Abbreviations

CERN	**C**onseil **E**uropéen pour la **R**echerche **N**ucléaire
EOS	**E**quation **O**f **S**tate
LHC	**L**arge **H**adron **C**ollider
LQCD	**L**attice **Q**uantum **C**hromo **D**ynamics
QCD	**Q**uantum **C**hromo **D**ynamics
QGP	**Q**uark **G**luon **P**lasma
RHIC	**R**elativistic **H**eavy **I**on **C**ollider
STAR	**S**olenoidal **T**racker **A**t **R**HIC

List of Symbols

α_s	coupling constant
η	pseudo-rapidity
γ^{dir}	direct photons
π	pion
ϕ	the azimuthal angle
ϕ_{p_T}	the azimuthal angle of a particle
ρ	density
μ_B	chemical potential
ψ_{EP}	angle of the event plane
θ	scattering angle
b	The impact parameter
P_T	transverse momentum
q	anti-quark
r_N	radius of nucleon
R_{AA}	Nuclear modification factor
$\sqrt{S_{NN}}$	Cetner of mass energy of colliding particles
T_c	Transition temperature
v_2	elliptic flow
v_n	the n-th harmonic co-efficient
V	potential

Chapter 1

Introduction

At the first millisecond after the Big Bang, matter existed in a special state called the Quark-Gluon plasma. This is a unique state in that the conditions necessary for its existence have not been met in nature since then. In this chapter, we introduce necessary concepts in particle and nuclear physics that allow us to discuss the QGP in some detail at the end of this chapter and the next.

1.1 Before the Standard Model

It can be safely generalized that by the early 1930s, the common consensus in scientific circles identified atoms as being made up of protons, neutrons and electrons, those being the most fundamental particles of nature.

In spite of the fact that the photon had already been discovered, there was no universal theory to tie the photon as a particle to the electron, proton, and neutron.

The theories available back then though, faced some serious challenges, chief among them is what holds the nucleus together. Back then, the only known force acting between protons inside the nucleus was the electromagnetic force. According to classical Electrodynamics, the presence of charged protons would imply the presence of very high repulsion by the electromagnetic force making the nucleus extremely unstable. This contradicted with our knowledge of the world in which the nucleus, by and large is stable except in special cases.

This and other discrepancies were studied by theoretical physicists of the time. The process that has been long led to a series of discoveries throughout the twentieth century where more and more particles were discovered. The study of all those particles as well as how they interact is organized into a theory called the Standard Model.

1.2 The Standard Model

In short, the Standard model is a theory that aims to firstly categorize all elementary particles, and secondly study and describe how those particles interact with each other. According to the standard model, all matter is made up of particles called fermions. Forces on the other hand

are carried by another family of particles called bosons. In it's entirety, the standard model is therefore a study of both fermions and bosons.

1.2.1 Fermions

Fermions are particles with the characteristic of half-integer spin values. Fermions obey the Pauli exclusion principles in that no two identical particles in one quantum system can obey the same quantum state at the same time. At the most fundamental level, the two most elementary fermions are quarks and leptons. While historically protons and neutrons for example have been called elementary particles, developments in Particle Physics have proved that in fact quarks and leptons are the true elementary particles of matter. This is due to two reasons. First of all, both particles are very small so as not have any known structure. Quarks and Leptons are so small that they behave as points in space or less than 10^{-18} metre. This is about 1/1000 the size of a Proton. Secondly, interacting together, they make up the more complex structures that we know. Protons and Neutrons for example are made up of Quarks. Electrons are in fact types of Leptons, so electrons are elementary particles.[1]

Quarks

Quarks are half-spinned particles, and there 6 distinct types of quarks. Their names are up, down, strange, charm, top and bottom. One of the important properties of the quarks is that they carry electric charge that is smaller than the charge of electrons and protons (-e and +e respectively). That is, up quark and down have a charge of 2e/3 while down strange and bottom have a charge of -e/3. Quarks also possess a property called color charge that has nothing to do with the normal colors that we see in day-to-day life, but is a property analogous to charge. This is going to be discussed in some detail later separately when we talk about the Strong Force. [1]

Leptons

As for Leptons, they come in charged and neutral categories. The charged ones carry a charge of -e; those are electrons, muons and taus. For each of those charged leptons there is a corresponding neutral one; the names of the neutral leptons being electron-neutrino, muon-neutrino, and tau-neutrino, and those as is obvious, carry no electric charge. A table containing all the leptons as well as their charge and mass is included in figure 1.1 [2]

1.2.2 Anti-fermions

In general, each particle has a corresponding anti-particle having the same mass of the particle but opposite electric charge and magnetic moment. A particle and anti-particle react together

Particle	Symbol	Mass (GeV)	
Electron neutrino	ν_e	0	
Electron	e	0.00051	First
Up quark	u	0.002 to 0.008	Generation
Down quark	d	0.005 to 0.015	
Muon neutrino	ν_μ	0	
Muon	μ	0.106	Second
Charm quark	c	1.0 to 1.6	Generation
Strange quark	s	0.1 to 0.3	
Tau neutrino	ν_τ	0	
Tau	τ	1.78	Third
Top quark	t	175	Generation
Bottom quark	b	4.1 to 4.5	

FIGURE 1.1: A list of quarks and leptons with their masses [3]

by annihilation (a reaction between a particle and anti-particle in which the two particles disappear releasing energy). The antiparticles of fermions are anti-fermions.[4][5]

Anti-quarks

Antiquarks are the antiparticles of quarks, and they have the symbol q. Just like quarks, they are half-spinned particles, albeit negative instead of positive spins in this case. The names of the antiquarks are anti up, anti down, anti strange, anti charm, anti top and anti bottom. Figure 1.2 shows all the antiquarks, their symbols, their charges, baryon and strange numbers.[6]

anti-leptons

Similarly, antileptons are the antiparticles of leptons. Similarly as well they have masses equal to that of leptons but opposite charges. The six antileptons are positron, anti-muon, anti-tau, electron anti-neutrino, muon-antineutrino, and tau anti-neutrino. Their symbols are included in figure 1.3 [7]

1.2.3 Bosons

In addition to the particles, the second domain of the Standard Model is forces or how those quarks and leptons interact. The four fundamental forces of nature are the strong force, the weak force, the electromagnetic force and the gravitational force. While the standard model

Particle	Symbol	Electrical charge	Baryon number	Strange number
Anti up	$\bar{u}$	-⅔	-⅓	0
Anti down	$\bar{d}$	+ ⅓	-⅓	0
Anti strange	$\bar{s}$	+ ⅓	-⅓	+1
Anti charm	$\bar{c}$	-⅔	-⅓	0
Anti top	$\bar{t}$	-⅔	-⅓	0
Anti bottom	$\bar{b}$	+ ⅓	-⅓	0

FIGURE 1.2: A list of antiquarks [6]

first generation	second generation	third generation
electron antineutrino $\bar{\nu}_e$	muon antineutrino $\bar{\nu}_\mu$	tau antineutrino $\bar{\nu}_\tau$
positron e^+	antimuon μ^+	antitau τ^+

FIGURE 1.3: A list of antileptons [7]

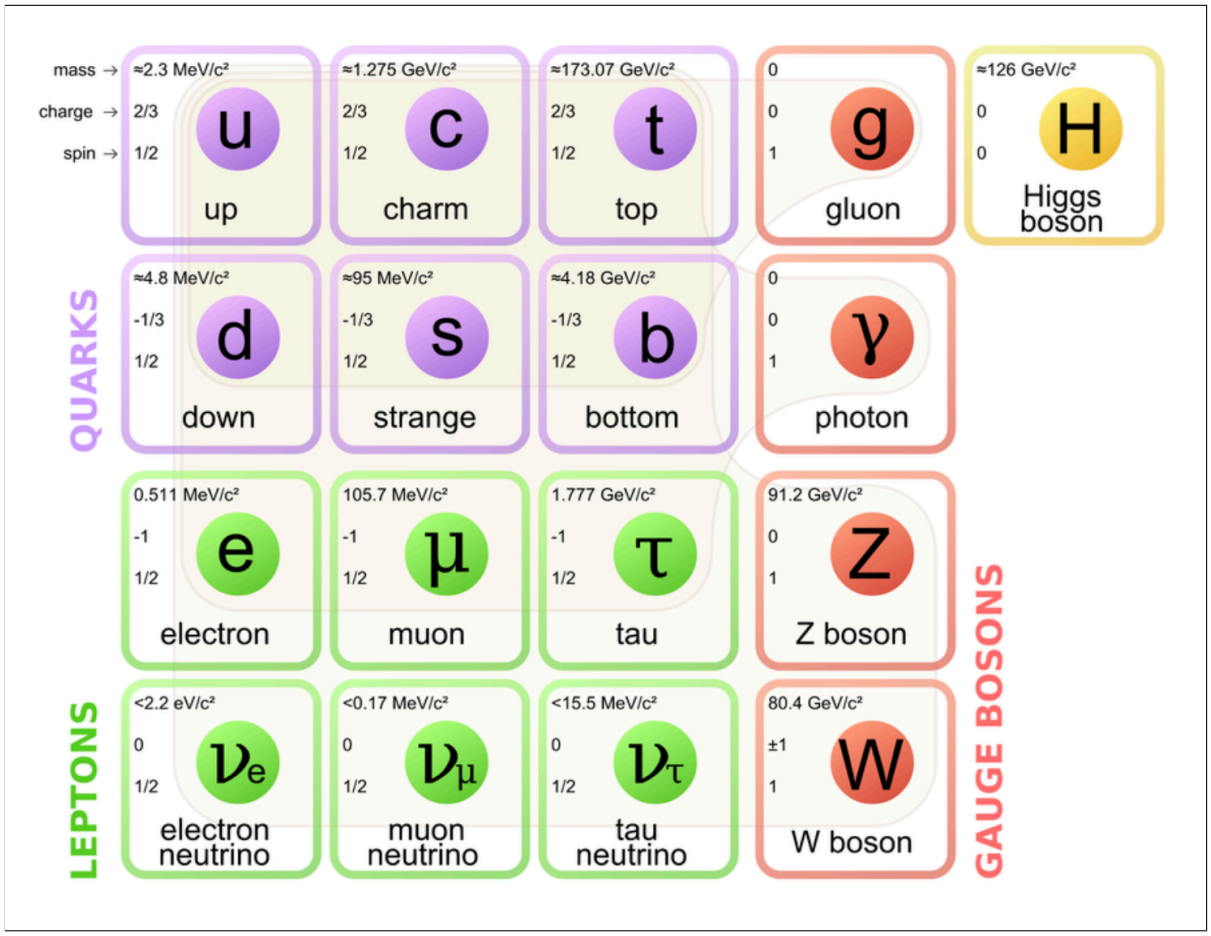

FIGURE 1.4: The Standard Model [9]

does not study the gravitational force, it studies the other three forces in detail, and how those forces act between fundamental particles to build more complex particles. According to the standard model, forces are the result of the exchange of intermediary particles between subatomic particles. The exchanged particles in the case of the strong force, the weak force and the electromagnetic force all belong to a family of particles called the bosons. In case of the electromagnetic force, this boson is the photon. The weak force is the result of exchange of the "W and Z bosons". And the strong force is brought about by the exchange of gluons. Graphical figure 1.4 summarises the standard model and as can be seen is divided into the quarks, leptons and bosons.[8]

1.3 The Strong Force

1.3.1 color

In the standard model, the force that acts between quarks causing them to bind into more complex structures is the Strong Force. In general, the strong force is a force that happens between particles carrying a property called color that is analogous to electric charge. Just as the electromagnetic force happens between particles carrying charge, the strong force happens between particles carrying color charge.

Of the two families of subatomic particles, quarks and leptons, quarks are the ones that carry color whereas leptons are colorless. Therefore the strong force acts between quarks and not between leptons.

Now what is the messenger particle responsible for the transmission of the Strong force - after all as has been mentioned above, according to the standard model forces happen due to the exchange of particles? The particle responsible for the transmission of the Strong Force, happens to be the gluon.

And what the strong force acting on quarks does is that it binds quarks together into more complex structures called hadrons. Hadrons are of two types, baryons and mesons.

1.3.2 Baryons

Baryons are heavy subatomic particles made of 3 quarks. Because each quark has a spin of half, baryons are half-integer spinned. Both protons and neutrons are baryons, where protons are made up of 2 up quarks and one down quark, while neutrons are made up of 2 down quarks and one up quark. The baryonic composition of a system is usually measured by the baryon number, where the baryon number is the number of baryons minus the number of anti-baryons of a system. Figure 1.5 is a figure of a nucleus having a number of protons and neutrons. The figure shows the quarks inside the protons and neutrons [10].

1.3.3 Mesons

Other than the baryon, the other type of hadron is the meson. A meson is made up of a quark and anti-quark held together by the strong force. In general the mesons are unstable, lasting between 10^{-22} up till 10^{-8} seconds only ultimately decaying to other stable particles namely electrons, neutrinos, and photons. [12]

1.3.4 Confinement

One of the properties of the strong force is that it acts on a very small range. How small? about 10^{-15} metre, which is equivalent to the diameter of a proton or a neutron. This of course

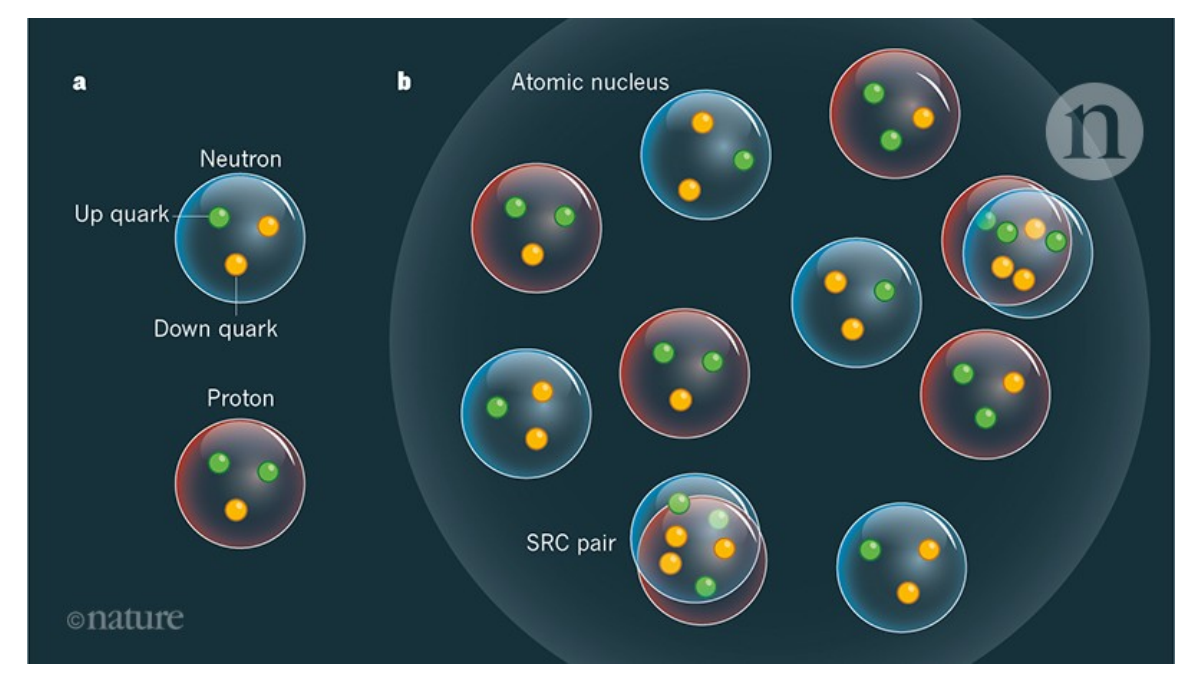

FIGURE 1.5: Quarks in protons and neutrons inside a nucleus [11]

explains why it was only discovered when subatomic particles began to be studied and not before that.

Now one interesting fact about the gluons that differentiates them from say photons for example is the fact that gluons have color whereas photons don't have charge. Therefore gluons are not only the mediators of the strong force, but are also particles on which the strong force acts. Due to this unique property, the strong force increases as the distance between two quarks increases, and does not decrease as is the case of electromagnetic force.[13]

What happens though as the energy of any of the bound quarks starts increasing? While the force maintains its strength as the distance increases, after a certain threshold, the force becomes big enough for a quark to separate. As it separates though, all this available energy, gets converted into anti-quark particles, and what ends up separating are quark-anti-quark pairs.[13]

The result of this fact is what is called confinement; quarks never exist alone but always exist bound up in baryons or mesons. As has been explained above, even when energy is provided the energy-gaining quarks separate from whatever bonds they're in as quark-anti-quark pairs.

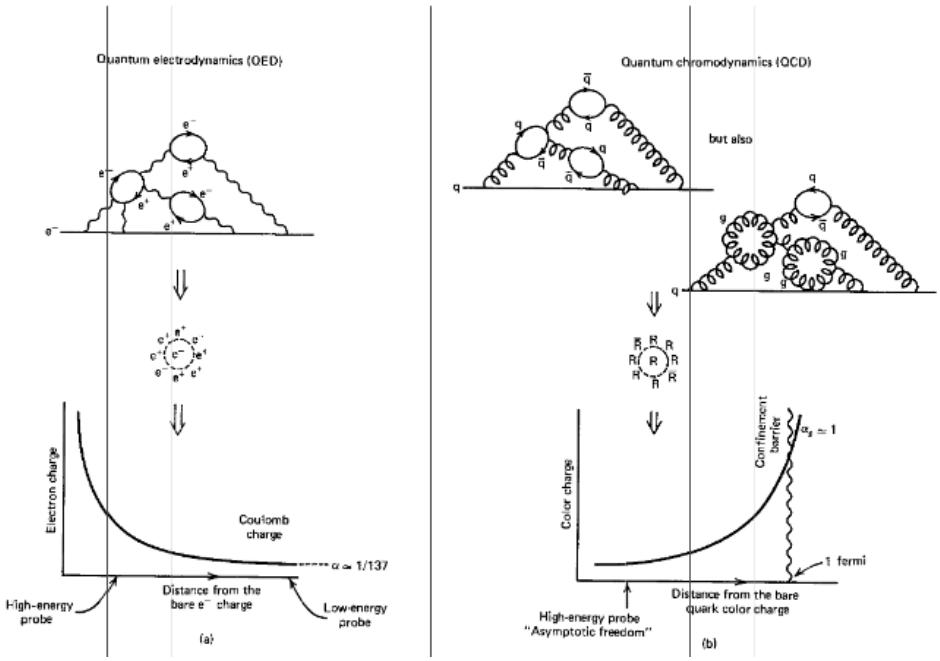

FIGURE 1.6: Confinement and asymptomatic freedom [14]

1.3.5 Asymptomatic Freedom

Does this mean that there is no way at all of studying a quark, without having to study the anti-quark with it, is there no remote or archaic case in which the quark exists alone, in a non-confined state?

Well fortunately the answer to this question turns out to be yes, there does exist a case in which the quark isn't confined. As quarks get very close to each other; to within separation distances smaller than the diameter of a proton, exchanging gluons decreases. At a small enough distance, the exchange of gluons almost stops, and the quarks stop feeling any forces from other quarks or gluons. This state is called the state of asymptomatic freedom, and provides us with the following (overly-simplified here) recipe to study quarks with no forces on them; if you want a free quark, squeeze matter rather than expand it![13]

1.4 Quark-Gluon plasma and early universe

Quarks that exhibit asymptomatic freedom exist in a plasma like structure called the quark-gluon plasma. In short thus, the quark-gluon plasma is a very dense special plasma in which quarks and gluons are swimming freely. The temperature required for matter to get converted into this plasma state is phenomenally high as would be shown in next chapter. It was just in the first microsecond after the big bang, that the temperature was high enough for matter to exist in this state. And between this early age of the universe and now, no natural conditions

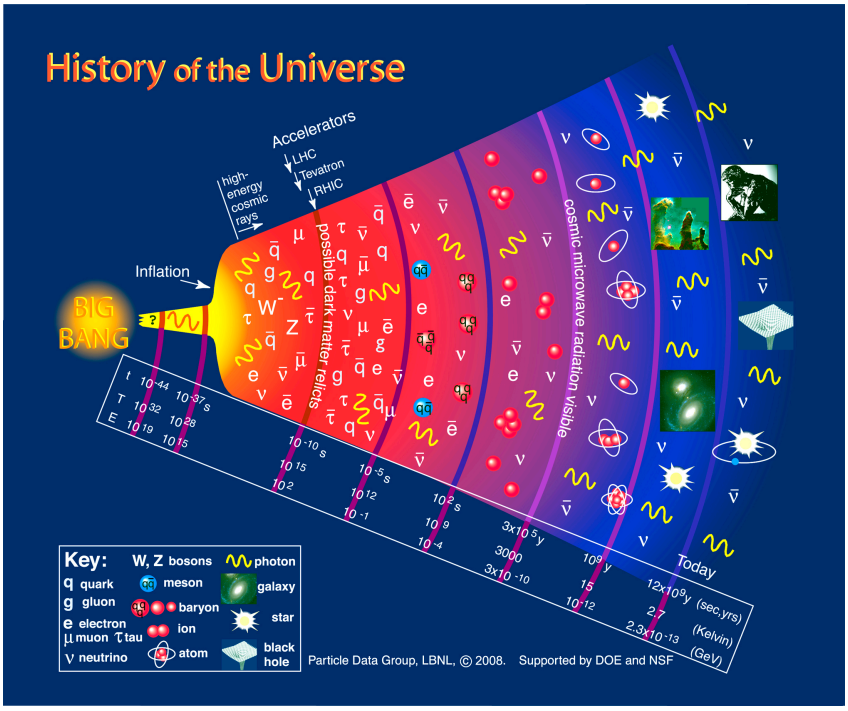

FIGURE 1.7: Timeline of the early universe. Quarks and gluons exist freely in first phase. This is the Quark Gluon plasma[15]

have existed to allow for the formation of this plasma. This makes studying this plasma very difficult. And while normally we're able to get earlier images of the universe through the use of strong telescopes that capture images of the universe light years away (and thus well into the past), we don't have strong enough tools to be able to look at the first microsecond after the creation of the universe. This is where high energy collisions come into focus. In high-energy collisions, the energies to which the colliding particles are accelerated are high enough, leading us to suspect the possibility of formation of QGP for a very brief period after a collision. By utilising and studying those collisions therefore, we're able to both infer whether or not the QGP is in fact created, and the secondly to study it.

1.4.1 Applications of Quark-Gluon plasma physics

An important question has to be addressed here before we get into additional details. Building heavy-ion particle accelerators and running experiments for understanding the quark-gluon plasma are extremely expensive endeavors. What possible benefits could then justify those very heavy expenditures? What do expect to gain by studying something as archaic as the quark-gluon plasma? Listed below are some of the expected benefits:

- While nucleons dominate the mass of atoms, the mass of the three quarks making up either a neutron or a proton makes up less than 1% of the mass of each of those nucleons

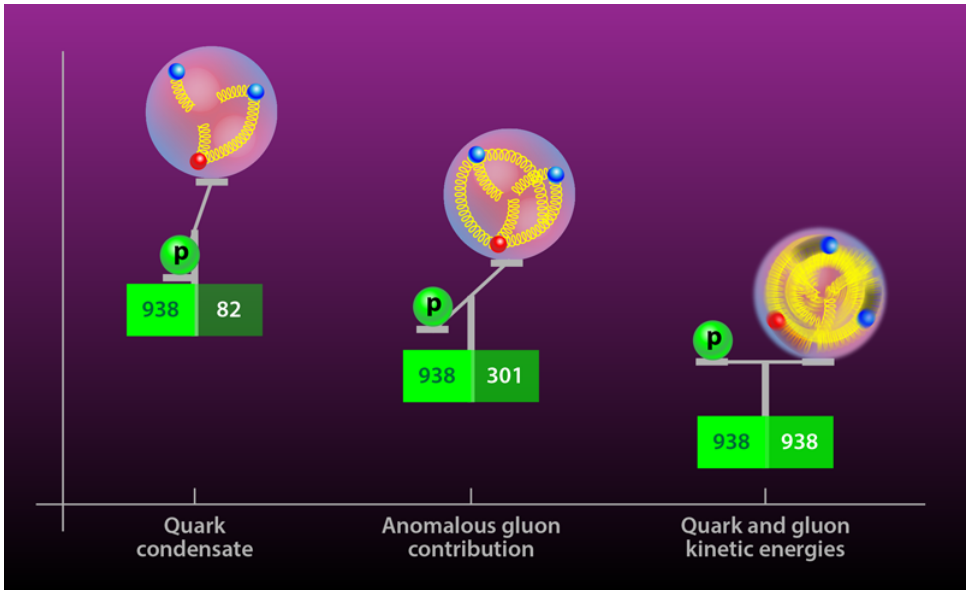

FIGURE 1.8: The mass of quarks make up less than 1% of the mass of the proton [16]

according to some estimates (for example a proton is made up of one up quark and two down quarks. The mass of those 3 quarks is less than 1% the mass of a proton as shown in figure 1.8). This means that the field tying those nucleons together is what makes up most of the mass of the nucleon.

Since the nucleus is made up of nucleons, and since the mass of an atom is concentrated in its nucleus, we can see that this field is what dominates the mass of all matter. Studying this field therefore by melting hadrons thus might allow us to answer the question of what is mass? [17][18][16]

- In the universe around us, quarks and gluons exist almost entirely in confined states. The universe itself is made up of a big vacuum in which matter exists almost entirely in this form; quarks confined up in hadrons. QGP is the only exception that we know to this confinement rule. Creating QGP therefore allows us to study matter in a form that we simply have never known before. [17]

- Quarks come in 6 flavors, up down, strange charm, top bottom. In QGP plasma, the strange charmed, and bottom quarks are formed abundantly. Those 3 flavors in particular aren't usually abundant in other experiments or natural conditions. Studying the QGP thus allows us to study not only those particular flavors that are hard to study otherwise, but would allow us to answer the deeper question of what exactly is flavor? [17]

- Because QGP was the state in which matter existed in the first seconds after the Big Bang, following which, matter started cooling down, to form matter as we know it, studying

the QGP allows us to

  - Understand how normal matter formed from QGP plasma.
  - Compare this knowledge to the models that we have built about the Big Bang, to verify those models and improve them. [17]

- As is going to be discussed in more details later, in heavy-ion-collisions, new quarks are formed, and this precipitates the transition into the quark-gluon plasma. In essence, the energy from the collisions is used for the creation of those new quarks. Again this in essence is, the transition from energy into matter. This again is one more reason to study the physics of QGP; as understanding it allows us to understand how energy is transformed into matter, and more importantly, can allow us to understand if its possible to turn matter into energy. [17]

Chapter 2

Background

In this chapter, the concepts on which this thesis was built are explained. The aim of this chapter is to give an overview about the abstract ideas that were used in the context of this thesis. The goal is to lay the necessary ground-work needed for explaining the methodology and the algorithm that are presented at the end of this chapter.

2.1 Physics of De-confinement

As has been discussed above, due to confinement the conditions necessary to break quarks out of their confined states are extreme conditions. Quarks exist in either quark-anti-quark pairs, mesons, or as three quarks bundled together, baryons. Either of the resulting particles is called a hadron. In order to understand how can we get from the hadronic phase to the Quark-Gluon-Plasma, the effect of pressure and temperature on hadrons have to be discussed. Then the term chemical potential is introduced and its relation to phase transition is discussed.

2.1.1 Asymptomatic freedom and pressure

To understand the relationship between asymptomatic freedom and pressure, first we examine the formula connecting V, the potential between quarks, as a relationship to r, the distance between them. This relationship is given by:

$$V(r) \approx= \frac{-4\alpha_s}{3r} + kr$$

Here k is constant, but α_s, that is called the coupling constant is proportional to r. Therefore as r increases, the effect of the second term dominates, and the potential increases linearly with r. On the other hand, as r decreases, the potential decreases.

Now we happen to know that the Baryon number is a conserved quantity (the number of baryons minus the number of anti-baryons). This means that increasing the density, has no effect on the number of baryons in the system. Therefore increasing the density leads to

a decrease in the distance between two nucleons (since we are sure that no baryons would vanish in the process of increasing the density to keep the baryon number conserved)

Since the radius of a nucleon, r_N, is about $1fm$, a decrease in the distance between nucleons so that the distance is less than $1fm$ leads nucleons to overlap. This happens at densities higher than $\rho = r_N^{-3} = 1fm^{-3}$.

When nucleons overlap, quarks crowd-up causing the distance between each to decrease considerably and the potential to asymptotically disappear, and we get what we call asymptomatic freedom.

Now since one way to increase this density is to increase pressure, thus squeezing matter together, it can be concluded that as the pressure increases the potential decreases, and thus asymptomatic freedom becomes easier to reach. [19]

2.1.2 Asymptomatic freedom and temperature.

Now we come to temperature, and look into the relationship between temperature and asymptomatic freedom.

In the past section we discussed the effect of density on de-confinement, and then went on to study the relationship between density and pressure and concluded that an increase in pressure would lead to enough increase in density that would in turn lead to de-confinement. We do the same here with temperature.

What happens when a dense hadronic gas is heated? We know for one that the mean kinetic energy per particle increases with the increase in temperature. In addition to this, and this is the crucial relation, the particle number increases, because while baryon number and lepton number are conserved, the particle number is not. Why though would the particle number increase?[19]

The strength of the force between quarks is determined by a factor called the coupling constant α_s that has been seen in the formula between potential and distance. As is obvious from figure 2.1 the coupling constant decreases with increasing momentum. [20]

As matter temperature increases and quarks gain energy the force between two quarks becomes weaker. This keeps happening as the temperature keeps rising until at high enough temperatures, the quarks break apart. In the breaking process, this available energy though, goes into the creation of new quark-antiquark pairs. As this keeps repeating, the density increases, and the distance between quarks keeps decreasing. And has been discussed above, as this distance keeps decreasing, the potential between the quarks keeps decreasing and eventually we get to asymptomatic freedom.

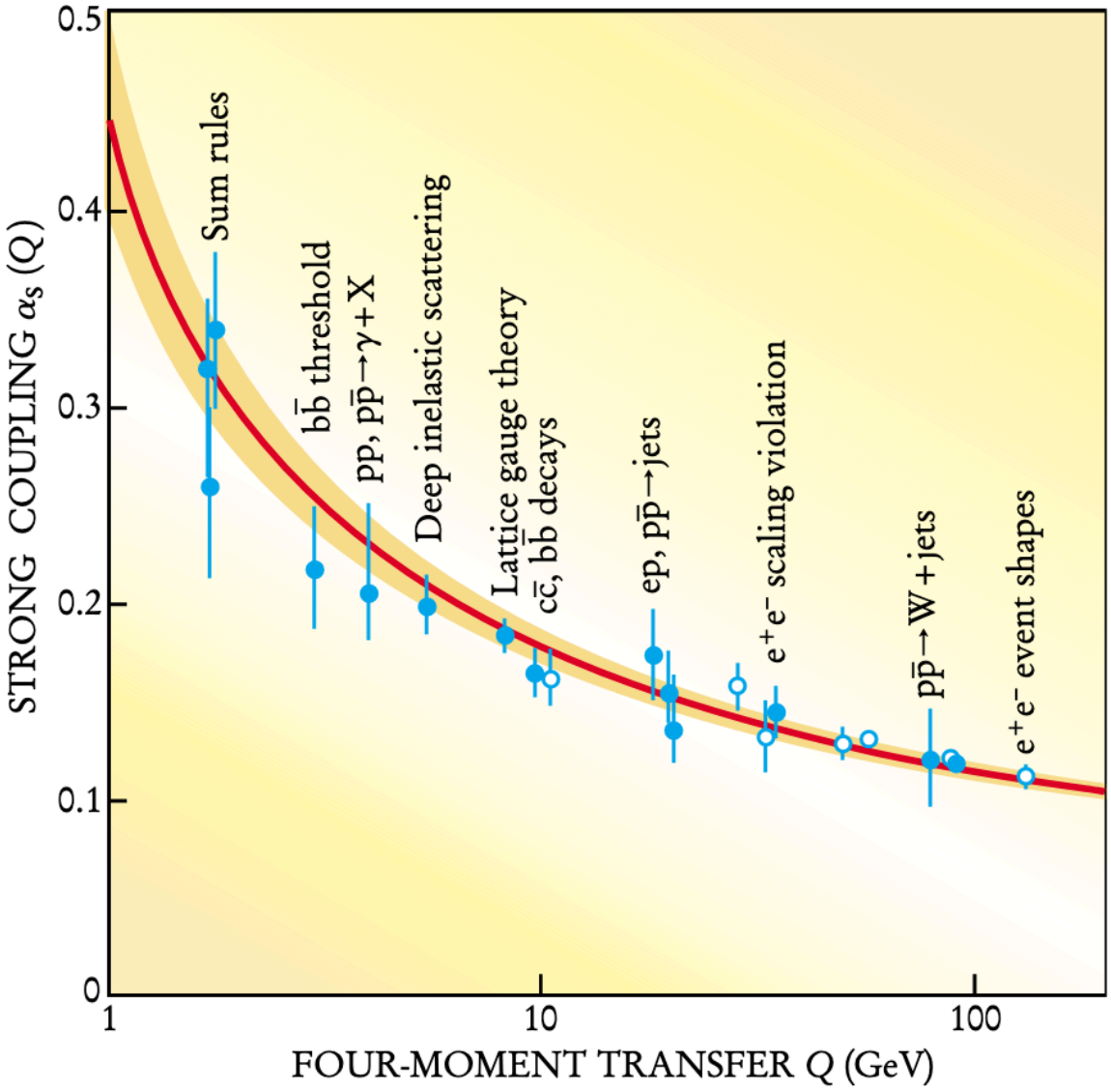

FIGURE 2.1: The running coupling constant decreasing with increasing momentum [20]

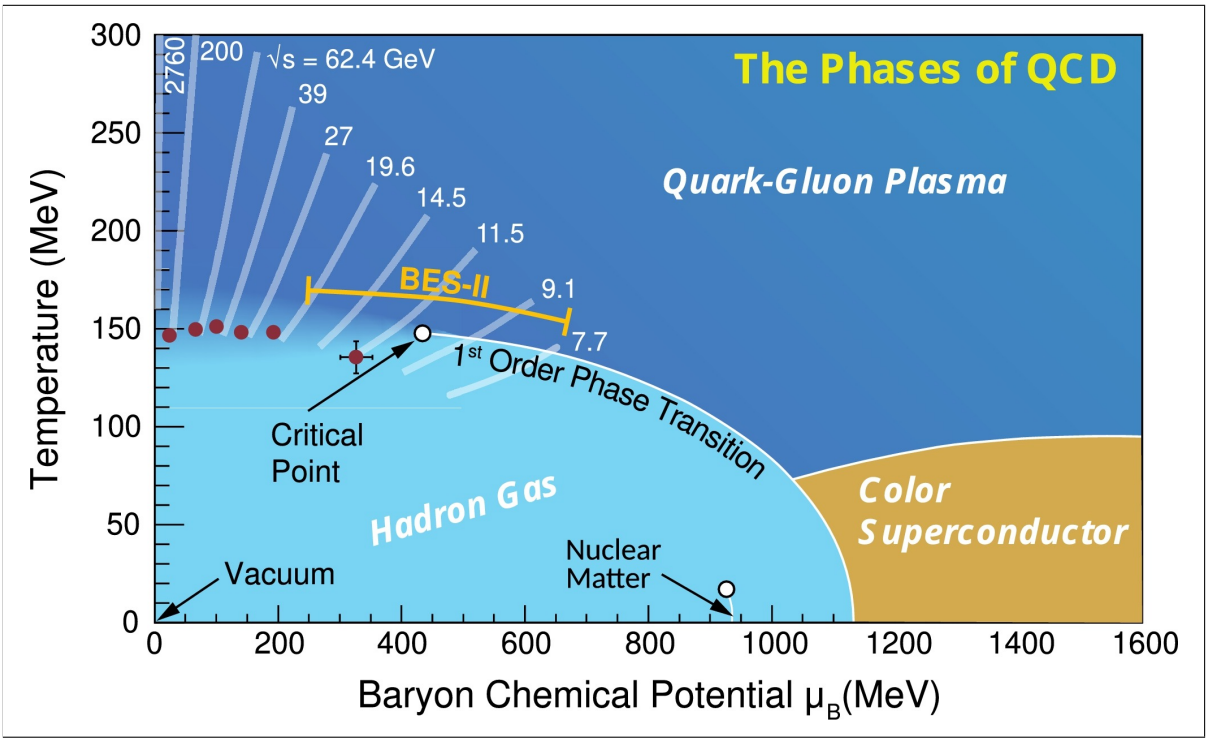

FIGURE 2.2: QCD phase diagram[23]

2.2 Chemical potential and phase transition

One other factor that needs to be included into any discussion of phase transition to quark gluon plasma is the effect of chemical potential on the transition. In short the chemical potential of any system, μ_B is the difference between matter and antimatter in the system. A chemical potential of zero indicates an equal number of baryons and anti-baryons. [21]

A diagram showing the relationship between chemical potential and phase transition is shown in figure 2.2. It's important to notice that at temperatures for RHIC experiments, the crossover does not happen at a certain temperature but over a whole region. Increasing the baryon potential in theory does eventually lead to a critical point where the cross over is over a single point. This is not the baryon potential in which RHIC experiments occur however.[22]

2.3 Calculating T_c using LQCD

As can be concluded by reading the previous section, we expect there to be a phase transition at high pressure and temperature. What we need to do here is to get an estimate of the temperature in which this could happen.

We know the Lagrangian in QCD to be

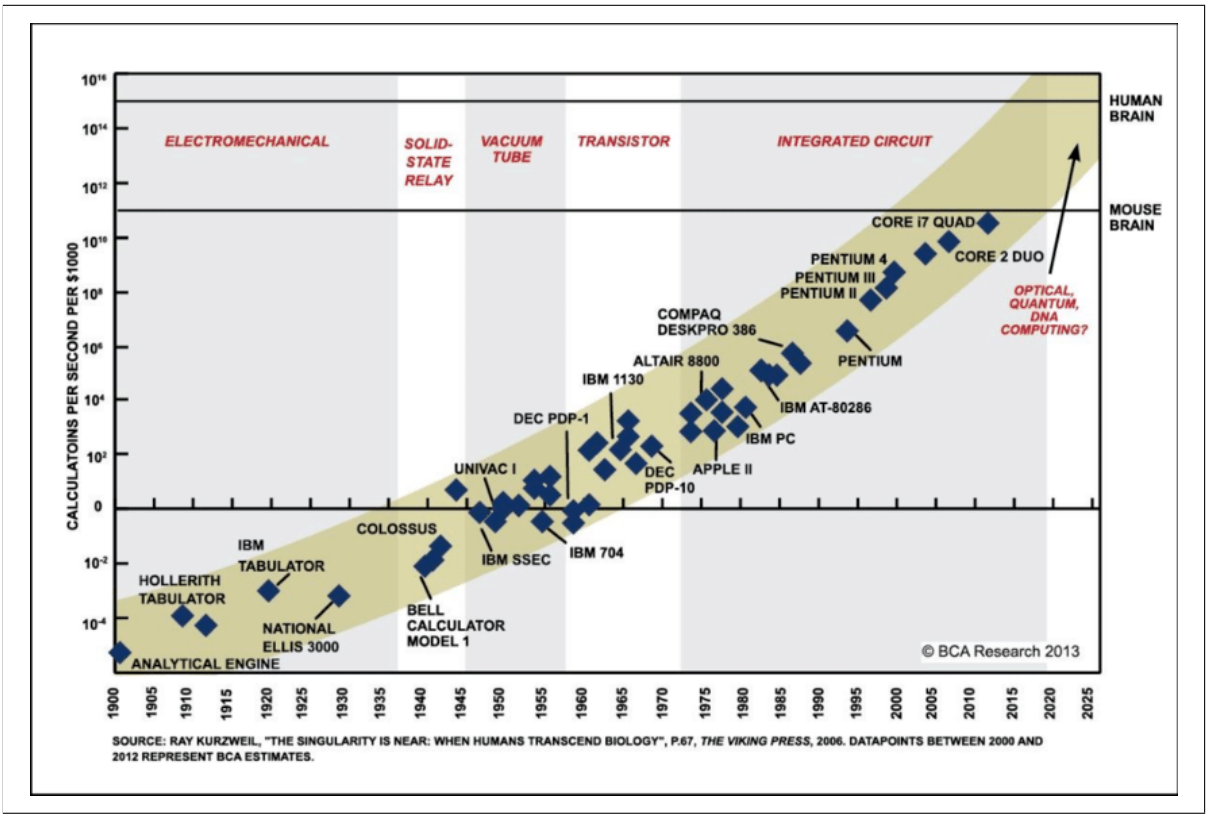

FIGURE 2.3: Moore's law

$$L_{QCD} = \psi_i(i\gamma^\mu(D_\mu)_{ij} - m\delta_{ij})\psi_j - \frac{1}{4}G^a_{\mu\nu}G^{\mu\nu}_a$$

Can this be used to calculate Tc, the transition temperature together with the many data points that we have to calculate the transition temperature?

Turns out that at high temperatures, we can use perturbation to solve this equation. Around the transition phase however, the quarks and gluons react so strongly that perturbative calculations become impossible. We can however make use of Lattice QCD, a numerical method to help us calculate the transition temperature.

Lattice Quantum-Chromo-Dynamics, LQCD, is a numerical non-perturbative method used to reach approximate solutions to QCD problems. While Lattice QCD is very expensive computationally, the more computational power that we have the more that we can infer. Just in the early 2000s the computational power became strong enough for us to infer from Lattice QCD, that the transition actually happens in a crossover region, rather than at a simple point. Figure 2.3 is a graph of Moore's law. The advances in computational power is what made Lattice QCD possible.[24]

Lattice QCD calculates the crossover region to start around 145 MeV and to have an upper

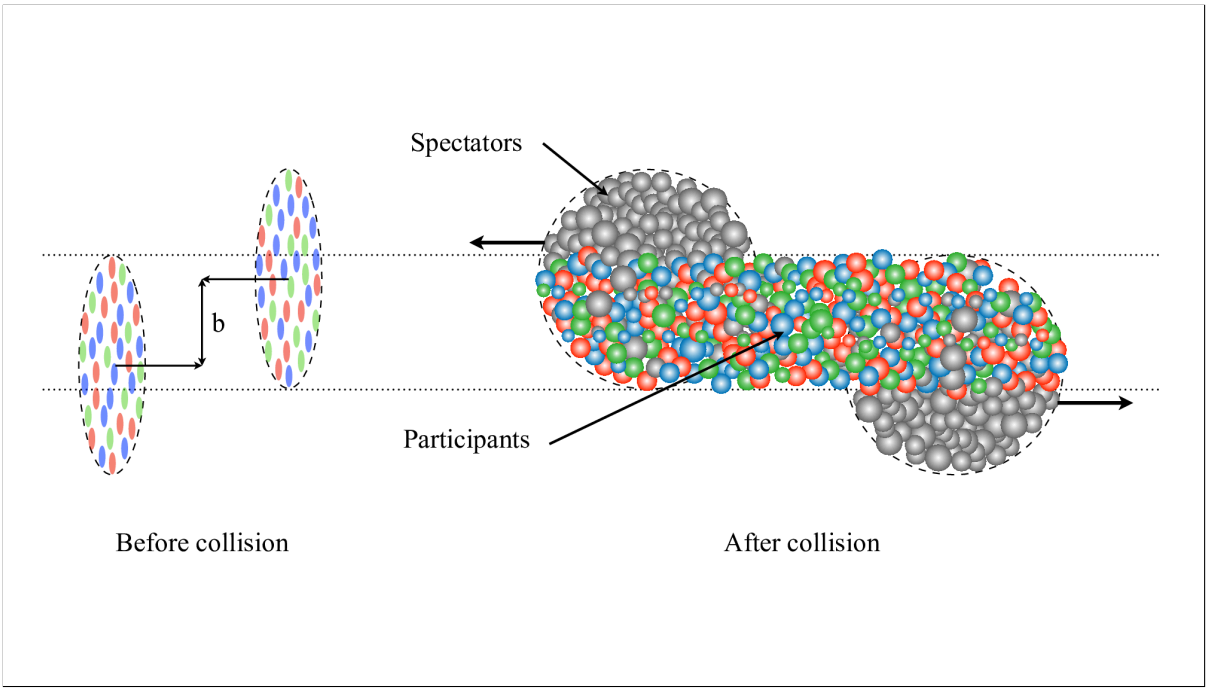

FIGURE 2.4: A schematic of a heavy-ion collision [26]

limit at about 170 MeV. In order to compare with the energies of the colliders we use the upper value[22]

$$T_c \approx 170 MeV$$

Since the energies of the heavy-ion colliders are $200GeV$ and $13TeV$ we have strong reason to expect the formation of QGP as a result to those high-energy collisions

2.4 The Physics of the collision

There are only two operating Heavy Ion colliders currently in the world. The first is the RHIC (Relativistic Heavy Ion Collider) in Brookhaven running at center-of-mass energy of $200GeV$, and the other the LHC (Large Hadron Collider) in CERN running at a whopping $13TeV$

2.4.1 Important parameters in studying collisions

Before getting into the classification of the collisions, we must first detail some of the parameters that are used in describing and studying those collisions. Figure 2.4 shows a diagram of heavy-ion collision helping illustrate the kinematics of the collision [25]

- The impact parameter b: The closest distance between two atoms if there was no interaction between them.
- The scattering angle θ: The angle of particle deflection after the collision
- The azimuthal angle ϕ: While θ represented the scattering angle in a two dimensional collision, ϕ represents the scattering angle in plane perpendicular to the transverse axis
- The pseudo-rapidity $\eta = -ln[tan\frac{\theta}{2}]$ is an alternative way to represent the scattering angle
- The transverse momentum $P_T = \sqrt{p_x^2 + p_y^2}$
- $\sqrt{s}$ represents the total center of mass energy of the colliding particles.

2.4.2 Classification of Heavy Ion collisions

The impact parameter b is used to classify the heavy ion collisions. Collisions where b = 0, which means that the 2 nuclei overlap, are called central collisions. On the other hand, collisions with non-zero b are called peripheral collision. As b gets bigger, the number of produced particles from the collision, logically decreases, as this means that the interaction between the nuclei was weaker.[27]

2.4.3 Spacetime evolution

In this section we'll briefly discuss the time line of heavy ion collisions starting with heavy ion nuclei all the way to the creation of the Quark Gluon plasma and back to the re-hadronization after the collision.

In heavy ion collisions, beams of nuclei, usually of gold or lead, are accelerated to relativistic velocities towards each other. Just after the collision, the two colliding nuclei meld into a medium of ultra high energy, called a fireball. Now matter is in a state called glasma, in which there are patrons of nuclei valence quarks and pairs of sea quarks. This is the intermediate stage. Further fragmentation of the patrons leads to the creation of the quarks and gluons and now the matter is in the state that is called the quark gluon plasma.

This plasma then expands and its temperature decreases, until it reaches the QCD transition temperature. At this temperature hadronization occurs in which the de-confined quarks and gluons form hadrons. In those as we already know by now, quarks are confined. The temperature at which this process occurs is called the chemical freeze-out temperature, and at this temperature quarks had already been hadronized. Further cooling leads to reaching the kinetic freeze out temperature. At temperatures below the kinetic freezeout hadrons stop exchanging energy and momentum.[27][22]

Figures 2.5 and 2.6 are different schematic representations showing this evolution.

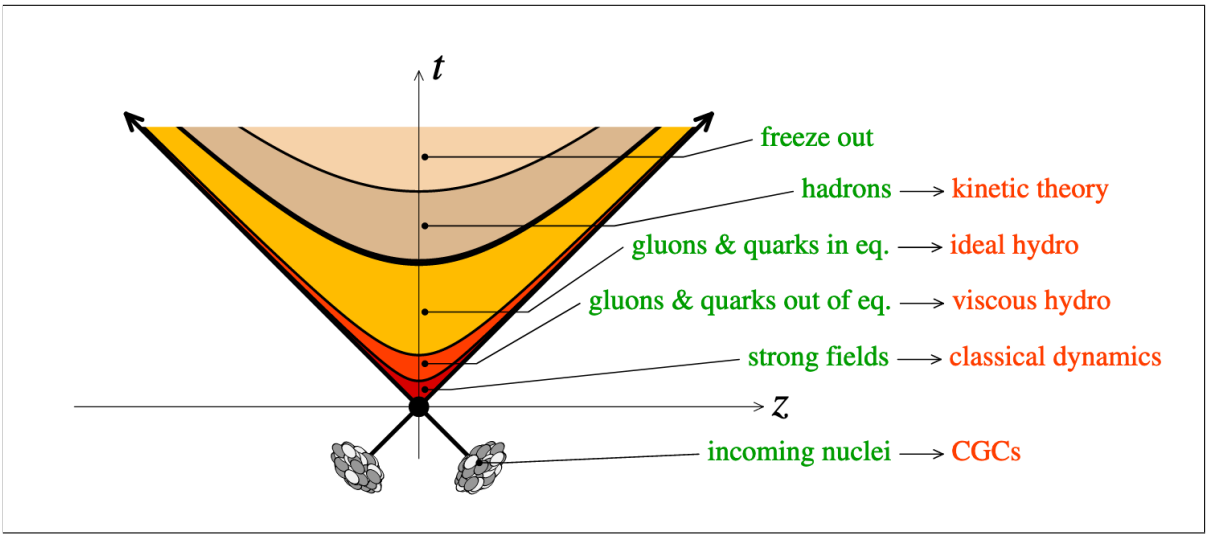

FIGURE 2.5: A schematic of a the space-time evolution of nucleus-nucleus collision [27]

Because all this process happens in a very short time, what ends up hitting the detectors in our accelerators are the hadrons that have reached the kinetic-freezeout phase. This is very important to note, because this means that while we only detect the hadrons at the detectors (we don't directly detect quarks or gluons), we work our way backwards in order to determine the presence of the QGP or to study it. In other words we must use results at the detector to draw conclusions about what happened in system between a collision and the detection process.

2.5 QGP Signatures

As has been mentioned in the previous section, because of the extreme conditions that are needed for the quarks to remain in non-confined state, QGP lives for very short periods of time. Detecting the formation of QGP is not done directly but indirectly using probes. In this section, we'd be discussing two of the most notable probes and those are jet quenching and elliptic flow.

2.5.1 Jet Quenching

Jets are traveling clusters of particles, say quarks or gluons. As they travel, they can lose energy and momentum, where the loss of energy and momentum depends on the nature of the medium in which they propagate and the nature of the propagating particles themselves. This loss of energy and momentum is called jet quenching, and for quarks and gluons is higher when traveling through Quark-Gluon-Plasma than when the plasma isn't created. Thus the

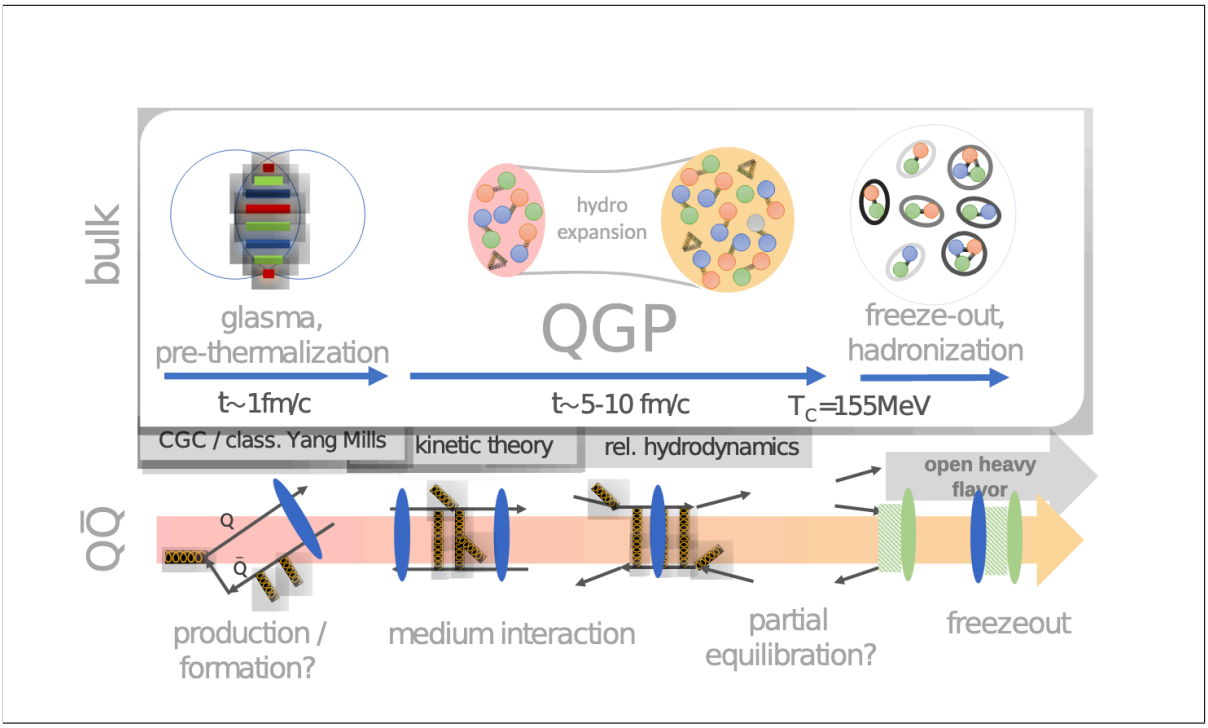

e

FIGURE 2.6: Different stages of heavy-ion collision [22]

presence of such quenching, specially the high loss is an indicator to the presence of the QGP. Jet Quenching is measured by a ratio called the nuclear modification factor, R_{AA} where the following formula is used to calculate it

$$R_{AA}(p_T) = \frac{dN_{AA}/dp_T}{N_{coll}dN_{pp}/dp_T}$$

where this basically is the number of particles being studied produced in nucleus-nucleus collisions to the expectation of particles created in proton-proton collisions[28]

Jet Quenching at RHIC and LHC

Figure 2.7 shows the R_{aa} of different produced particles in Au+Au collisions at RHIC as a function of transverse momentum. Figure 2.8 shows the R_{aa} of produced particles as functions of transverse moemntum at LHC in Pb+Pb collisions. R_{aa} for photons is almost 1. Similarly R_{aa} for W and Z bosons in figure 2.8 is also almost 1. On the other hand all the color charged particles that react to the strong force, have an R_{aa} well below 1, showing strong suppression. The suppression of reactive particles that react strongly to QGP but not particles that couple either weakly or electromagnetically is an indicator of the possibility of formation of QGP in high energy collisions.

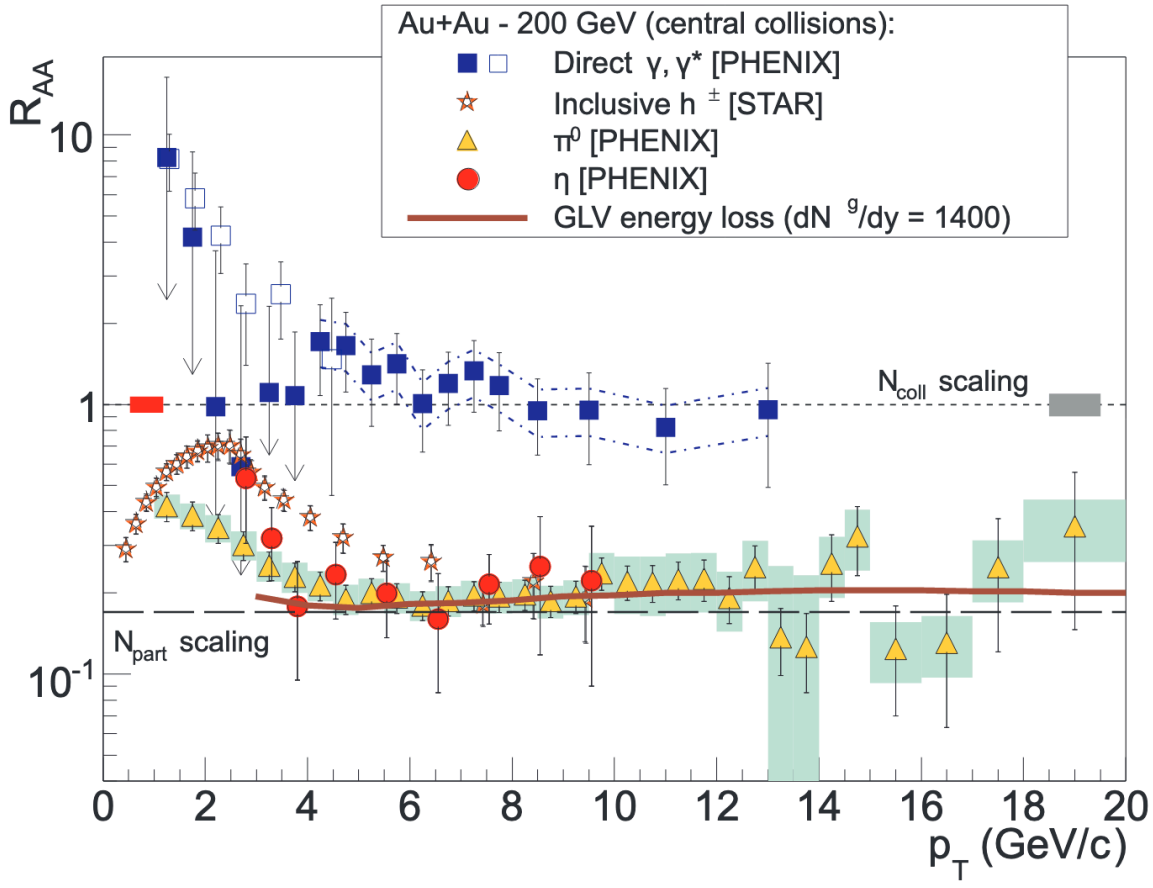

FIGURE 2.7: Measurements of $R_{AA}(p_T)$ from central Au+Au collisions at RHIC for different particles in addition to theoretical predictions [28]

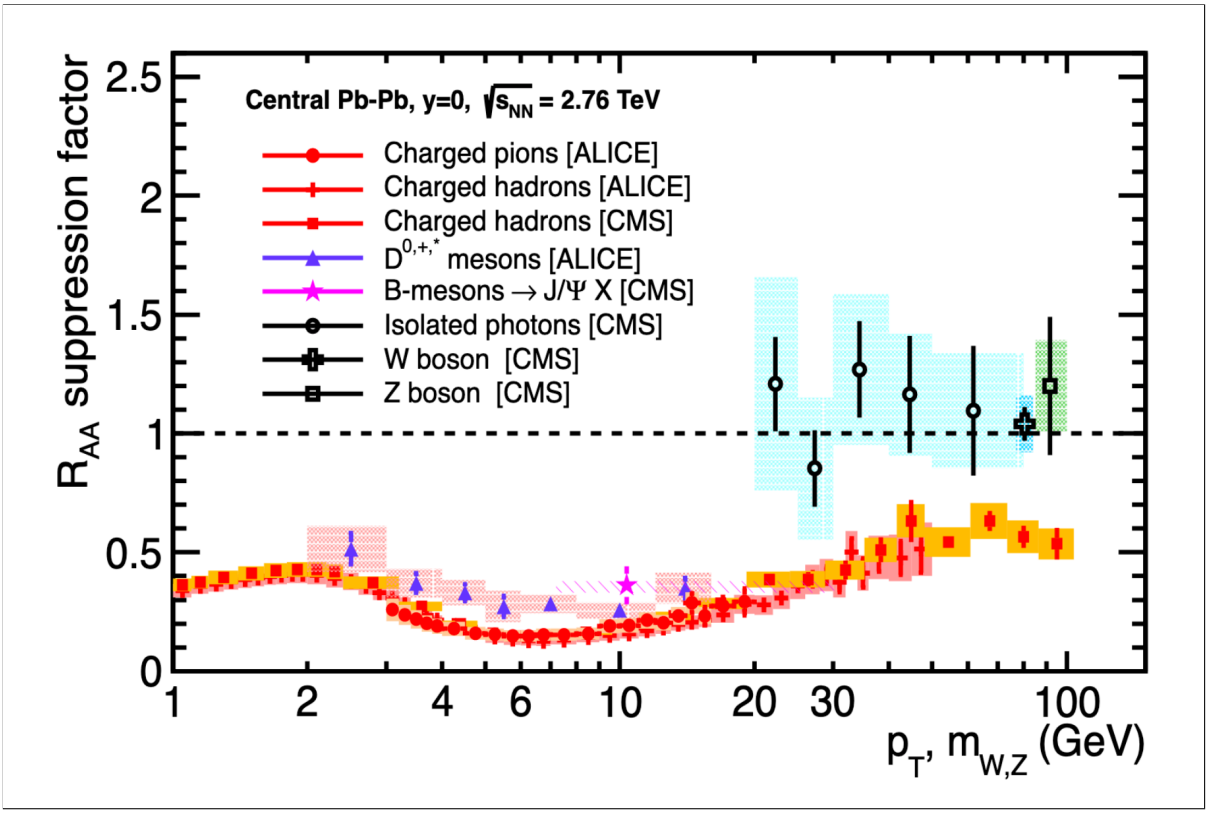

FIGURE 2.8: Compiled measurements of $R_{AA}(p_T)$ from central Pb+Pb collisions at LHC for different hadrons [29]

2.5.2 Elliptic flow

An alternative probe for determining the presence of QGP is Elliptic flow, v_2. In this section, the concepts behind v_2 calculations are presented as well as how v_2 could be used to indicate the presence of QGP.

Azimuthal anisotropy is the uneven distribution of momentum of particles with respect to the azimuthal angle from the reaction plane, and it measures the flow of the medium following the high energy collision. Here the reaction plane is determined by the impact parameter and the direction of the transverse beam. Figure 2.9 is a schematic showing a non-central collision of two nuclei, where the grey in the figure represents the reaction plane. [30]

The azimuthal distribution, is best quantified by expanding $dN/d\phi$ as a function of p_T in a Fourier Series [31]

$$\frac{dN}{d\phi}(p_T) = \frac{N}{2\pi}[1 + \sum_n v_n(p_T)cos(n(\phi_{p_T} - \psi_{EP}))]$$

Here ϕ_{p_T} is the azimuthal angle of a particle, ψ_{EP} is the azimuthal angle of the event plane, and v_n is the n^{th} harmonic coefficient

ψ_{EP} the angle for the event plane in turn is constructed as follows

$$\psi_{EP} = \frac{1}{2}tan^{-1}\frac{\sum_i sin(2\phi_i)}{\sum_i cos(2\phi_i)}$$

The second harmonic coefficient is what is called the elliptic flow, and can be represented by

$$v_2(p_T) = \langle\langle cos(2(\phi_{p_T} - \psi_{EP}))\rangle\rangle$$

where here the brackets denote statistical averages.

In the summation above, the second harmonic v_2, or elliptic flow is a dominant term. For this reason, v_2 is a good indicator of the azimuthal anisotropy.

Geometry of collision

In any collision, the number of particles taking part in the collision are called participants, while those not taking part are spectators (figure 2.4). The centrality of the collisions affects the number of the nucleons taking part in the collision, and thus the number of produced particles. The centrality is determined by the impact parameter described above, by the number of participating nucleons (a participating nucleon is a nucleon that took part in at least one inelastic collision) or the by the number of binary collisions. Figure 2.10(a) shows the the increase of the multiplicity of the produced particles with the increasing "centrality" of the collisions; in other words the number of produced particles increases with increased centrality. Figure 2.10

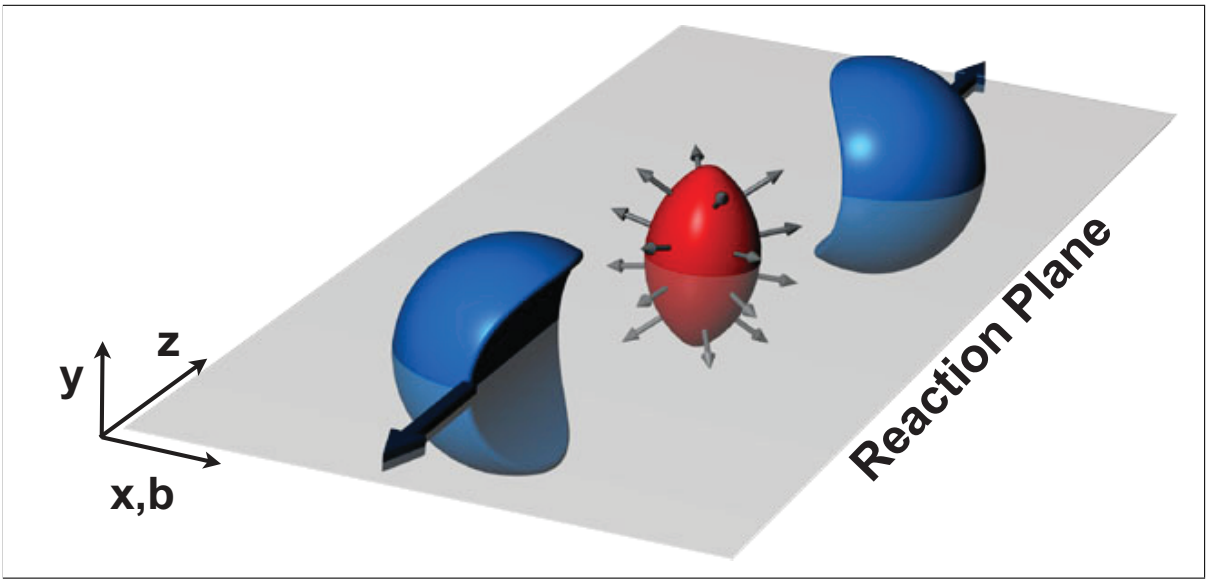

FIGURE 2.9: A non-central collision of two nuclei. The figure shows the uneven distribution of the produced particles in the event plane with respect to the azimuthal angle[30]

(b) shows the number of participating nucleons and the number of binary collisions in a Pb-Pb collision at center of mass energy $\sqrt{S_{NN}} = 2.76$ TeV and Au-Au at center of mass energy $\sqrt{S_{NN}} = 0.2$ TeV.[30]

The reactivity of the plane

As has been discussed above, we expect that at high enough momentum, for a brief period after collisions, QGP could be formed. Now, since quarks and gluons are color charged we expect different particles traversing a medium in which QGP exists to react to the medium (with strongly reacting particles showing the most couplin of course). This therefore leads to a bias of particles in the reaction plane. For instance, for particles like photons that react only electromagnetically to the plane, we expect very little reaction or coupling. Particles like W and Z pions, also only react weakly to the plane, therefore should show little reactivity. Color charged particles however should show high azimuthal anisotropy. It has therefore been theorized that azimuthal anisotropy at high P_T values can be explained by the presence of QGP in the brief seconds after the collisions. To validate this claim, azimuthal anisotropy for photons and pions can be compared to the azimuthal anisotropy of color charged particles. As the photons and pions weakly couple to the plane, and because photons in particular are final state particles that do not fragment into other particles, they are considered perfect guages detecting biases in the plane for reasons other than reactivity.

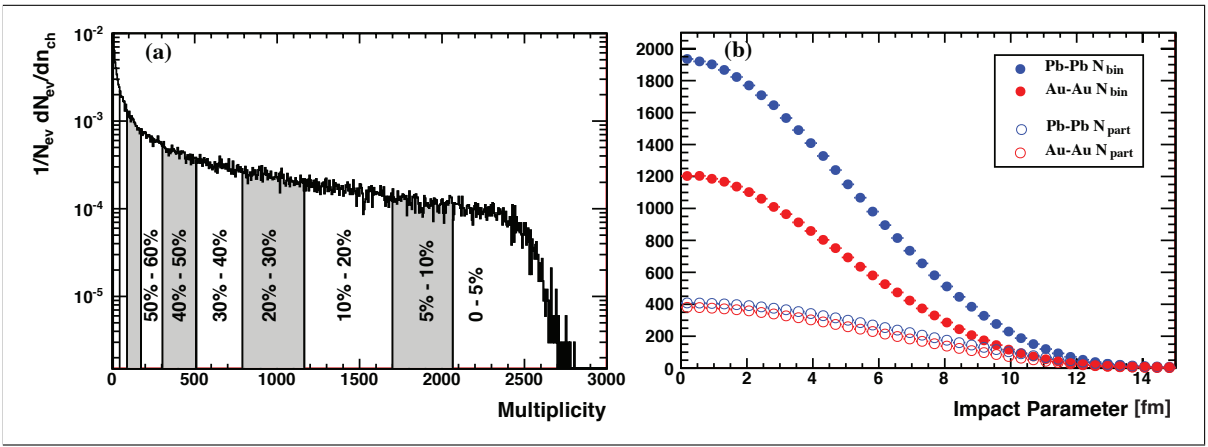

FIGURE 2.10: a) Charged particle multiplicity from Pb-Pb collisions at $\sqrt{S_{NN}} = 2.76TeV$. Imposed on the graph is the centrality of the collisions in the given bin b) Number of participating nucleons N_{part} and binary collisions N_{bin} vs. at different impact parameters for Pb-Pb collision at $\sqrt{S_{NN}} = 2.76TeV$ and Au-Au at $\sqrt{S_{NN}} = 0.2TeV$. (both taken from[30])

Thus in short, if QGP is formed, we expect this term, the elliptic flow v_2, to be significantly different at different values of p_T if the resulting particle from the collision is color-charged, and is thus reactive to the plane. In addition, the amount of anisotropy, should be proportional to the reactivity of the particle to the propagating medium. And this is the basis of the experiment or analysis that aims to detect the formation of QGP in high-energy collisions.[32][31][33]

Experimental measurements of v_2

In this section we present the experimental measurements of v_2 plotted against transverse momenta for collisions at both RHIC and the LHC. Superimposed on the the drawn graphs are plots of the predictions by theoretical models. Comparing experimental results to modeled results allows us to judge the strength of the models.

Figure 2.11 shows the v_2 distributions of different particles from the 200 and 130 Gev Au+Au collisions at RHIC. In the figure, results predicted by hydrodynamic models are shown in dashed lines. In figure (b) 2 models one assuming the creation of QGP (EOS Q) and the other assuming the presence of an ideal gas (EOS H) are compared to the experimental results. It can be easily observed the higher accuracy of the EOS Q in predicting the results. For the 2 models, a value of T_c is taken to be 165 MeV[34]

Figure 2.12 shows also the STAR results from RHIC but with a wider momentum range. As indicated in the caption, superimposed here as well are the results from the hydrodynamic models, used with the same parameters indicated above. While the previous figure contains results from models assuming the creation of QGP and ones that don't, the modeled data here limit themselves to the case where QGP is in fact created.[35]

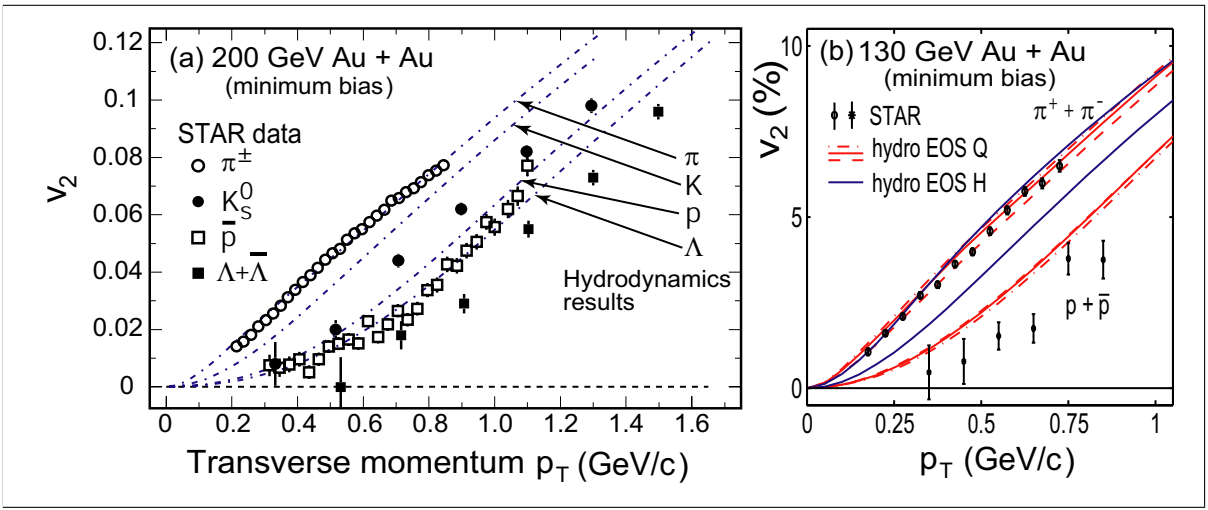

FIGURE 2.11: Elliptic flow vs. transverse momentum for different resulting particles in Au+Au collisions at 200 GeV. The calculations from hydrodynamic models are shown as well in dashed lines. (b) Experimental measurements of v_2 from STAR at center-of-mass energy 130 GeV. Superimposed on the graph are the calculations from 2 different hydrodynamic models, one assuming the creation of QGP (EOS Q) and the other in which no QGP is formed (EOS H). [34]

Figure 2.13 on the other hand shows the experimental results from LHC for different centrality bins. Again in this graph as in the figures for RHIC, modeled results are included in the graph. The parameters used for modeling are the same parameters used in the RHIC model described above.[35]

2.5.3 Methodology and Objective

As has been said, the goal of this study is to find ways to separate the effect on v_2 due to medium reactivity from the effect due to other factors that cause v_2 variance.

In this thesis therefore, we run simulations for proton-proton collisions at center of mass energies similar to those found at RHIC and LHC using Pythia. Since Pythia's simulation does not include the formation of QGP in its algorithm, those simulations give us a benchmark for comparison with the real experiment data. In other words, the aim here is to get the v_2 values that we expect to be produced for different particles after the collisions if no QGP is formed. The values available here thus would be the values of v_2 from already known forces (kinematics of the collisions for example). Before analyzing the real experiment data then, those values found here should be subtracted from the produced values. The resulting v_2 graphs after subtraction would then be used to infer whether or not QGP was formed.

Also, the graphs that are drawn are for 3 types of resulting particles from the collisions, photons, pions and heavy mesons. In real collisions the reactivity to the plane should differ based on the type of the resulting particle (as has been explained in detail above). In this study

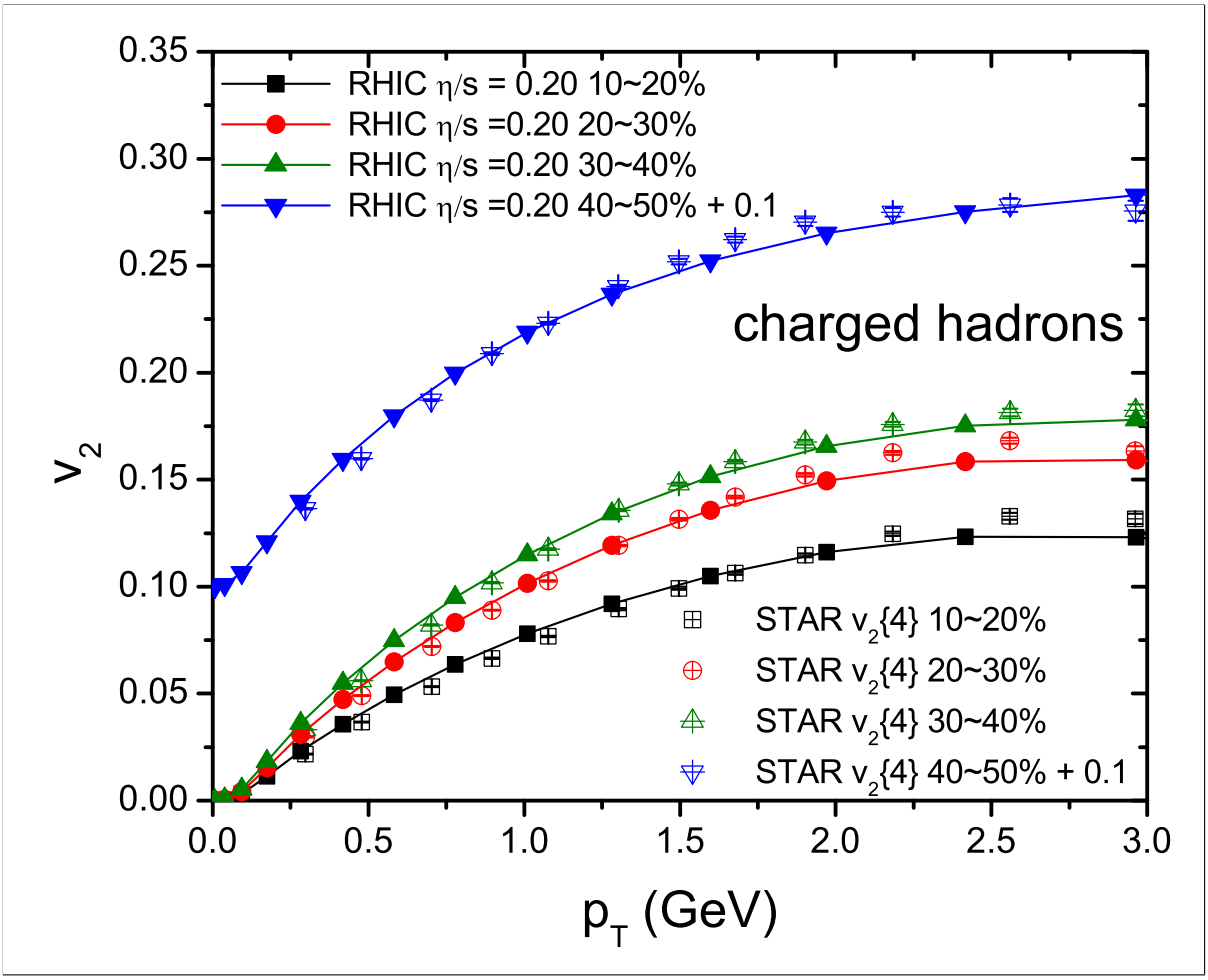

FIGURE 2.12: v_2 for charged hadrons from Au+Au collisions at $\sqrt{s} = 200$ GeV. The centralities are listed at the top left. Experimental data from the STAR experiment for $v_2(p_T)$ is shown with open shapes. The equivalent filled shapes are used to plot the data from the models. As can be seen the models are very accurate at predicting v_2 for transverse momenta shown in the graph[35]

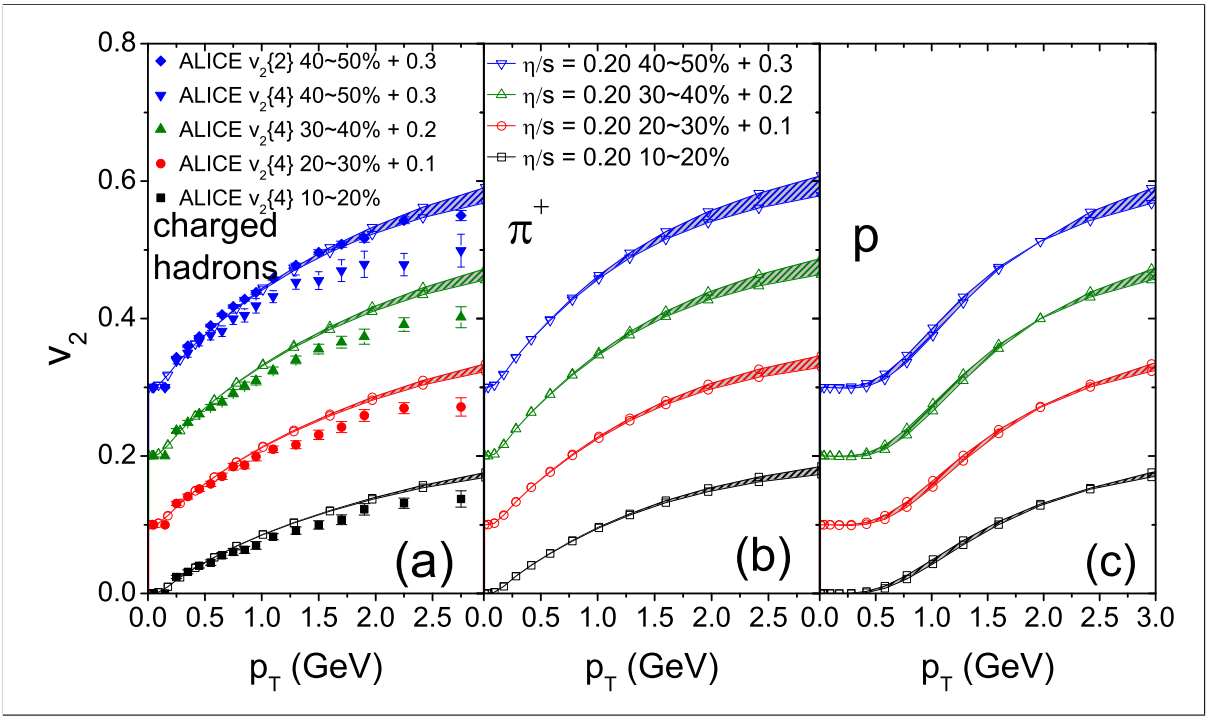

FIGURE 2.13: $v_2(p_T)$ for charged hadrons (a) pions (b) and protons (c), for Pb+Pb collisions of the indicated centralities at the LHC. Again here the experimental measurements are shown by solid symbols, while filled symbols are results from hydrodynamic models. [35]

then, we compare the results from those 3 graphs. The aim, is that since as has been mentioned above, for Pythia simulations no QGP is formed, any difference in the graphs of the 3 particles in this analysis should be accounted for when studying real world collisions. [32][31][33]

Chapter 3

Analysis and Results

In our analysis, we ran simulations of proton-proton collisions using PYTHIA 8 with its default parameters. The center of mass energy, $\sqrt{s_{NN}}$ was set once to 200 GeV-equivalent to the center-of-mass energy at which the collisions occurs at RHIC, and then the center of mass energy was set to 13 TeV corresponding to the center of mass energy at which the collisions occur at LHC. In PYTHIA, the deacay mode was turned on, to match the real physical experiments. This means that only the stable particles are recorded. The events are filtered so we choose the values of pseudo-rapidity η, where $-20 < \eta < 20$. All the values of ϕ though are allowed. In our simulation, a particle with p_T less than or equal 2 GeV is considered a soft particle, while that above that value is considered a hard particle. Only soft particles are included in the calculation of the event plane.

In this chapter we present the analysis and the results. We begin this chapter by a section on the necessary quality assurance of the produced data from the simulations. This is then followed by presenting and discussing the results.

3.1 Quality Assurance

3.1.1 Distribution of produced particles

Figure 3.1 and figure 3.2 show the frequency distributions of the produced particles per virtual collision (i.e: how many particles were produced in each virtual collision). Log scale has been used to capture small differences in the number of produced particles per event.

Figure 3.1 shows the frequency distribution of all particles for RHIC while figure 3.2 shows the frequency distribution for LHC. As can be seen the number of produced particles per collision for LHC is higher than that of RHIC. This is expected since the higher center-of-mass energy at LHC would lead to more particles being produced in each collision (event). [36]

3.1.2 Momentum distribution

In this section we present the number of produced particles for each bin of transverse momentum in both our simulations. The results are shown in figures 3.3 and 3.4 for simulations of

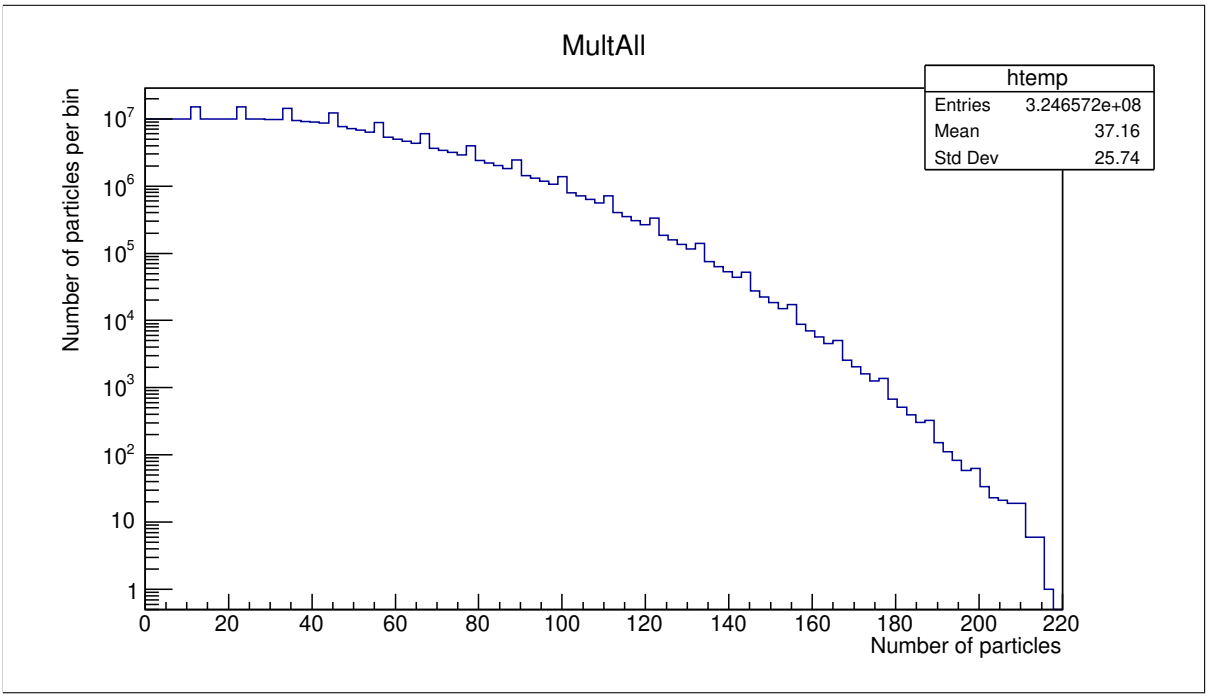

FIGURE 3.1: Distribution of the produced particles at $\sqrt{s_{NN}}$ = 200 GeV

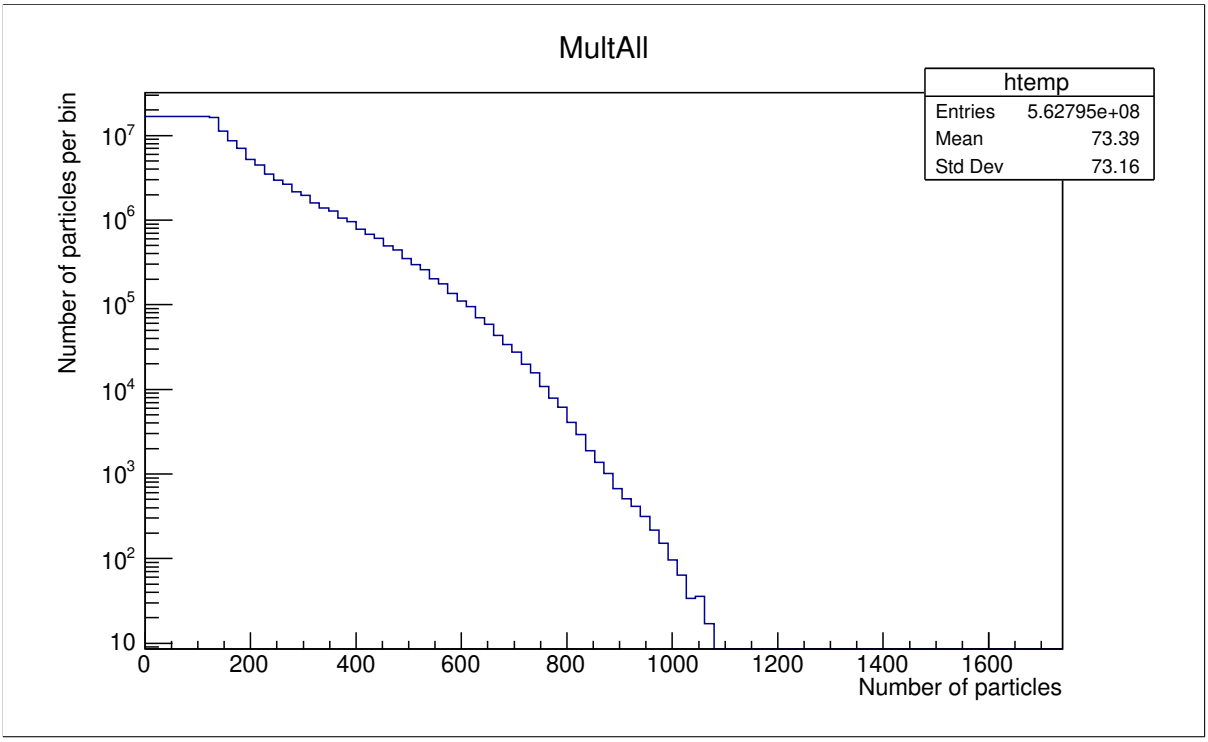

FIGURE 3.2: Frequency distribution of the produced particles at $\sqrt{s_{NN}}$ = 13 TeV

RHIC and LHC. As has been mentioned above, soft particles are particles with $p_T \leq 2$ GeV. The mean p_T is 0.315 GeV at $\sqrt{s_{NN}}$ = 200 GeV and the mean p_T is 0.308 GeV at at $\sqrt{s_{NN}}$ = 13 TeV. Those values show that in both collisions soft particles are the majority of produced particles. [36]

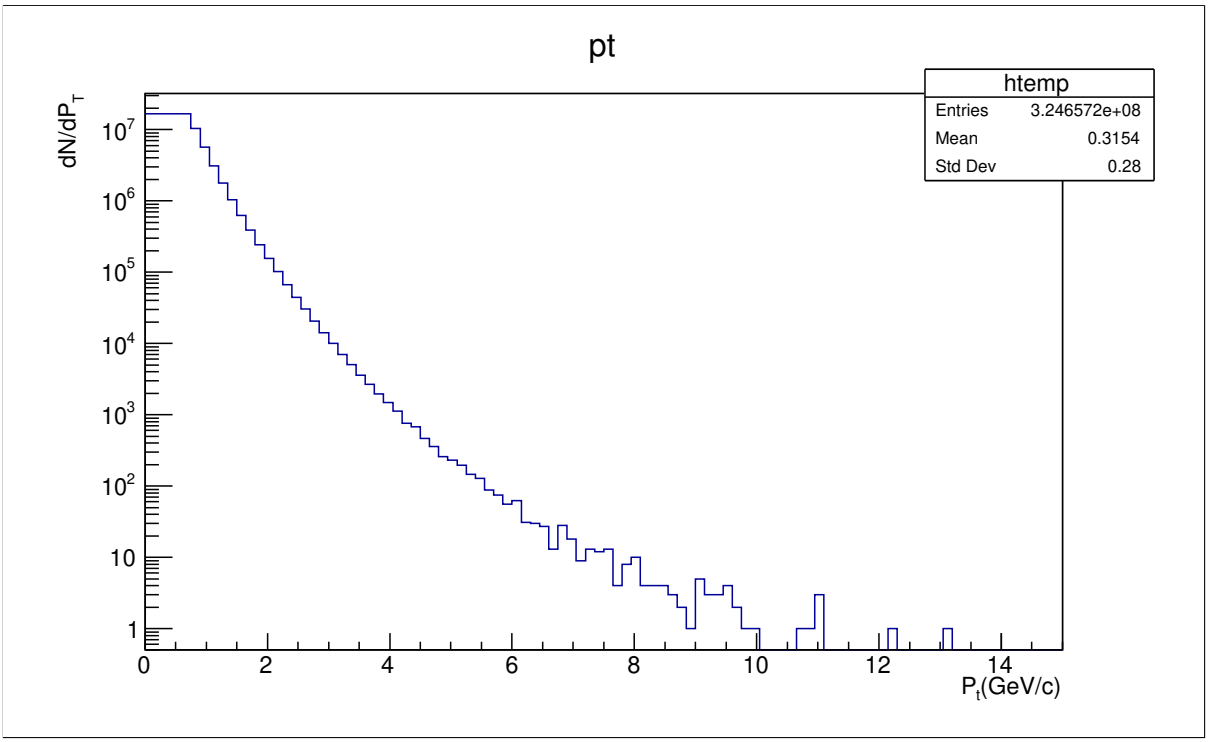

FIGURE 3.3: Frequency distribution of the produced particles at different transverse momentum bins at $\sqrt{s_{NN}}$ = 200 GeV

3.1.3 Pseudorapidity and Azimuthal distribution

The next four figures are histograms of the distributions of the pseudorapidity for RHIC and LHC then the azimuthal distributions for RHIC followed by LHC. As can be seen, the azimuthal distribution is uniform for all ϕ from -3 to 3 radians in both RHIC and LHC. The pseudorapidity is almost uniform in the range from -5 to 5, but then decrease afterwards for RHIC. This is similar to the pseudorapidity for the LHC similution, except for the fact that the range is wider; uniform from -10 to 10 to start decreasing afterwards. [36]

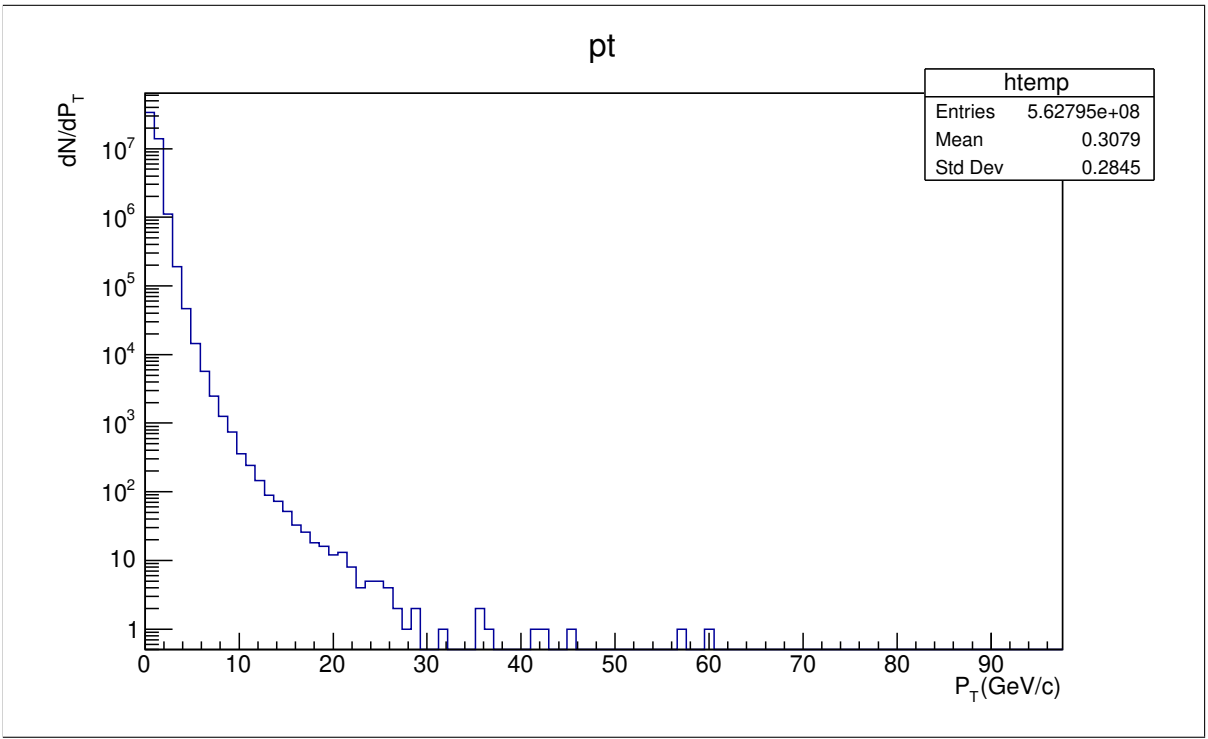

FIGURE 3.4: Frequency distribution of the produced particles at different transverse momentum bins at $\sqrt{s_{NN}}$ = 13 TeV

3.2 Analysis

As has been mentioned above, in our analysis, we ran simulations using PYTHIA at center-of-mass energies 200 GeV and 13 TeV for pseudo-rapidity range $0 < |\eta| < 20$. For each of the center-of-mass energies, we divide the pseudo-rapidity into bins, $0 < \Delta\eta < 1$, $1 < \Delta\eta < 2$, $2 < \Delta\eta < 3$, $3 < \Delta\eta < 4$, $4 < \Delta\eta < 5$, and $5 < \Delta\eta < 20$. This is done to avoid auto-correlation (particles in one pseudo-rapidity bin are much more likely to originate from the same collisions than particles in different pseudo-rapidity bins because of conservation of momentum). Then for each of the bins, we plot v_2 against p_T for direct photons, light mesons, and heavy mesons. By this, we aim to achieve two goals. First we're comparing the flow at different center-of-mass energies (the RHIC energy and the LHC energy), different quark flavors (direct photons are color-neutral while pions and heavy mesons would react to QGP), and different masses (pions and heavy mesons have different masses). This would allow us to learn the effect of each of those factors on v_2. The second and more important goal is that, as mentioned above, the obtained results would be used as probes to be compared to the real results obtained in the experiments. [36]

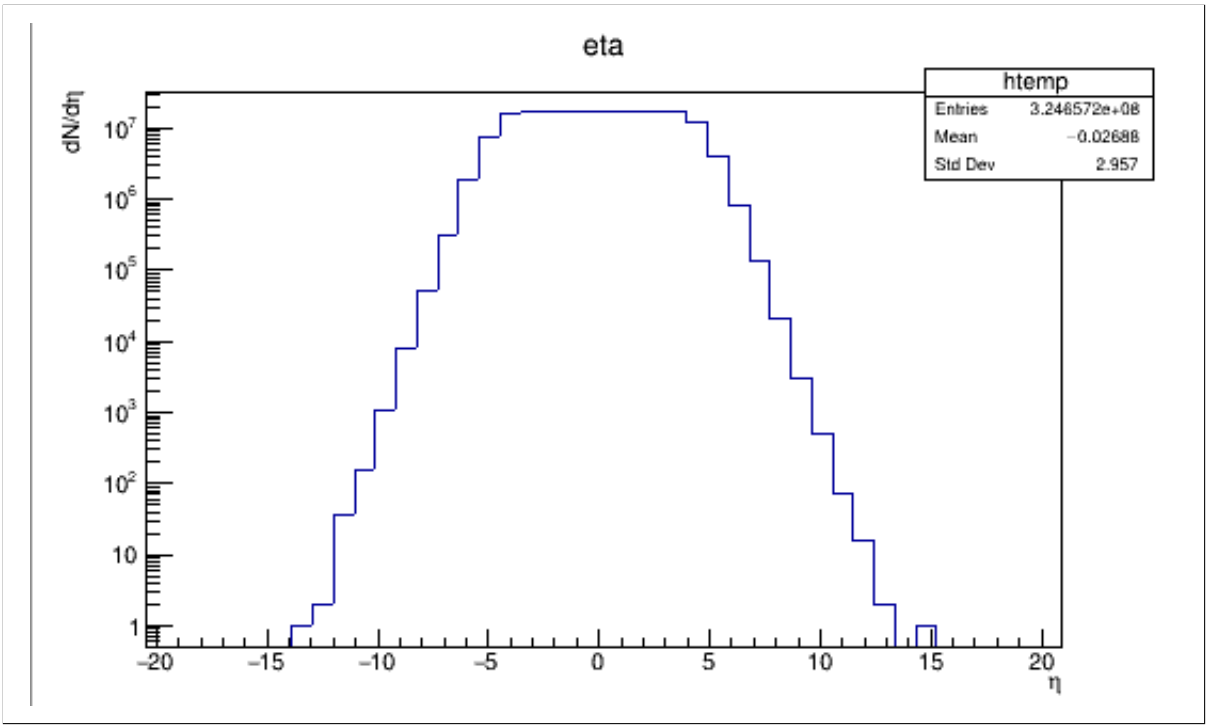

FIGURE 3.5: Pseudo-rapidity distribution of the produced particles at $\sqrt{s_{NN}}$ = 200 GeV

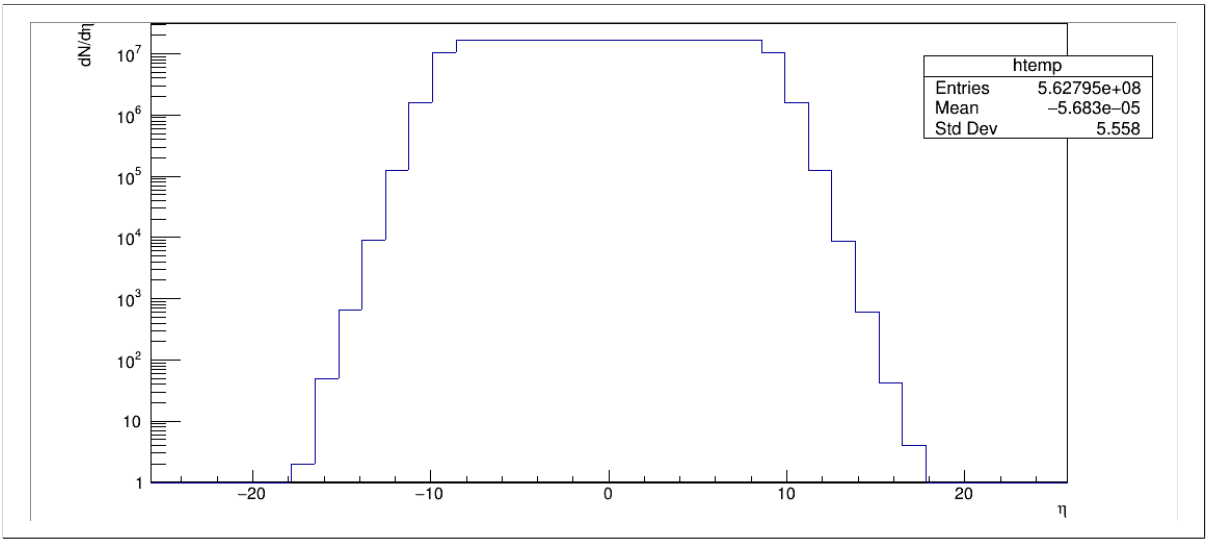

FIGURE 3.6: Pseudo-rapidity distribution of the produced particles at $\sqrt{s_{NN}}$ = 13 TeV

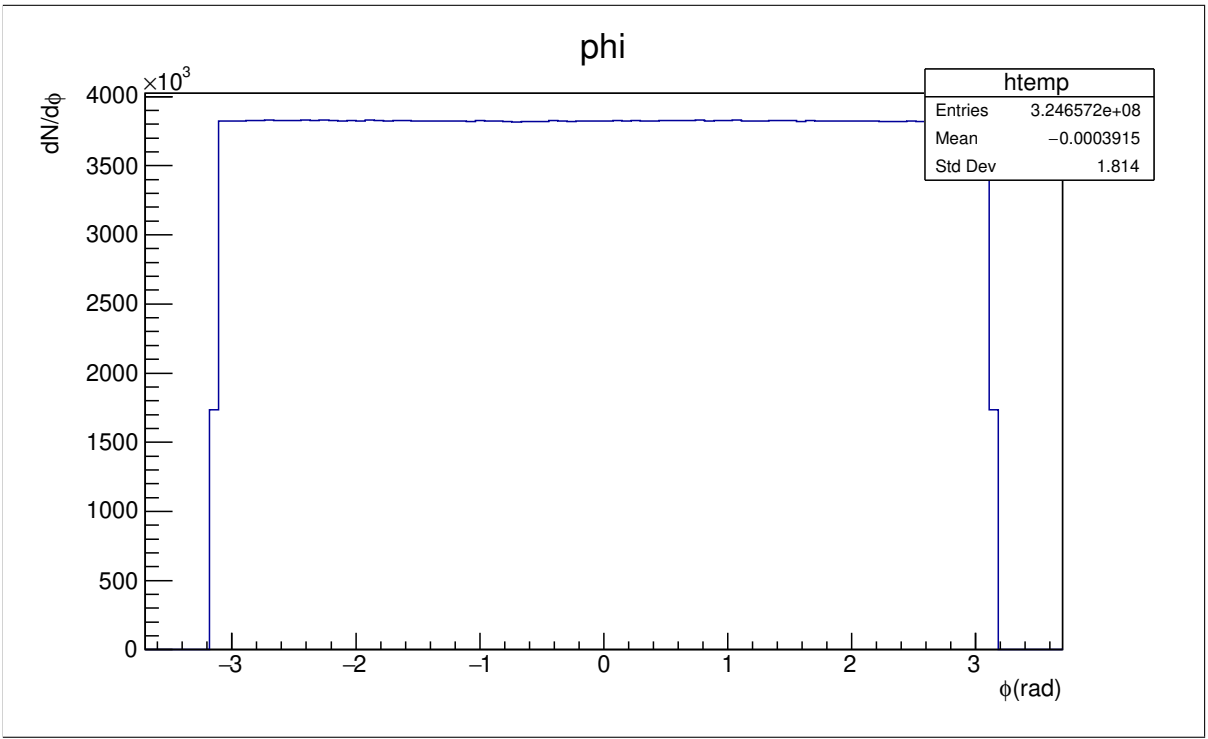

FIGURE 3.7: Azimuthal distribution of the produced particles at $\sqrt{s_{NN}}$ = 200 GeV

3.2.1 Expected results from theory

Given that in PYTHIA there is no final state interaction, in principle v_2 should be zero for the different particles at high p_T no matter the quark flavor. Also in PYTHIA, since no medium is formed, effects of surface bias emission would not exist. Whatever values received here thus of v_2, would act as probes to be compared to the experimental measurements of v_2.

3.3 Results

Figures 3.9, and 3.10 include the plots of v_2 against p_T. Figure 3.9 includes the results for center-of-mass-energy of 200 GeV and figure 3.10 includes the results for center-of-mass-energy 13 TeV. As has been described above for each of the center-of-mass energies, the pseudo-rapidity range is divided into bins. And each bin includes the v_2 for the pseudo-rapidity range of that bin for each of the particles; photons, pions and heavy mesons.

3.3.1 Effect of $\sqrt{S_{NN}}$ on v_2

Observing figures 3.9 and 3.10, and by comparing the value of v_2 at $\sqrt{S_{NN}}$ = 200 GeV and $\sqrt{S_{NN}}$ = 13 TeV for the same type of particle and $|\Delta\eta|$ bin, one can observe the effect of $\sqrt{S_{NN}}$

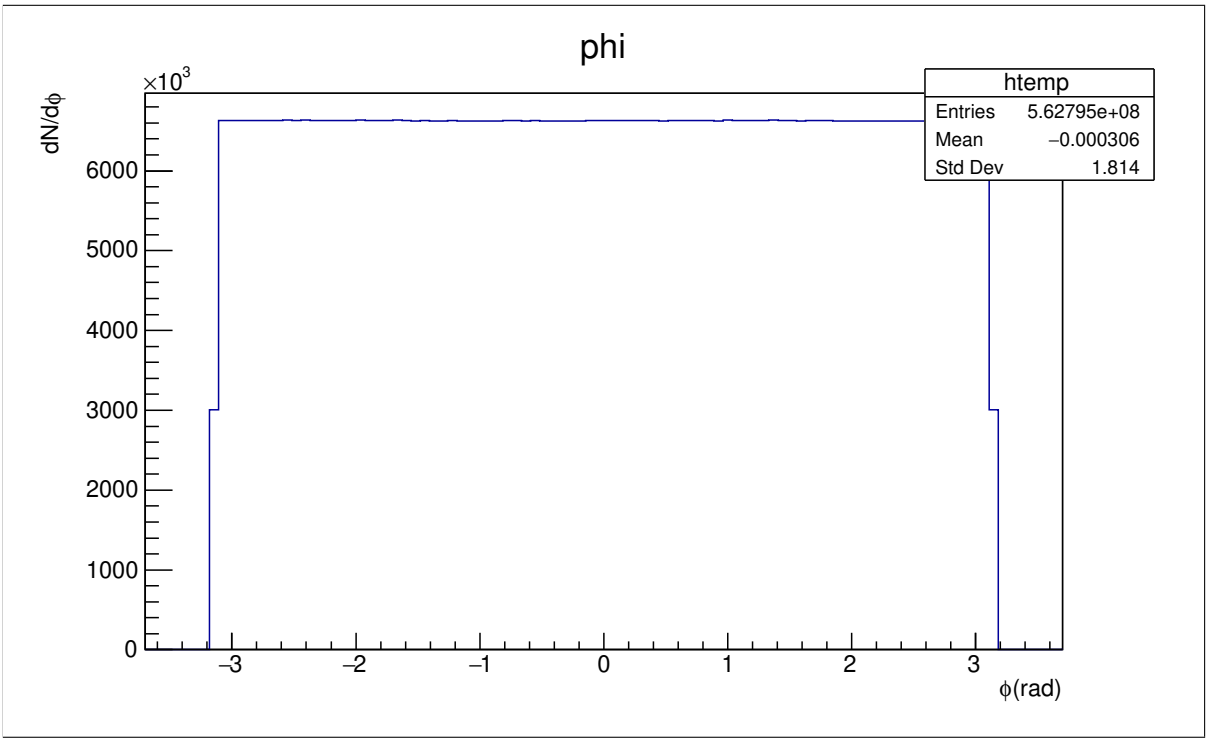

FIGURE 3.8: Azimuthal distribution of the produced particles at $\sqrt{s_{NN}}$ = 13 TeV

on v_2 due to non-flow contributions. The general trend is that value of v_2 is higher at the lower energy. The effect is more obvious for lower $|\Delta\eta|$ bins since the value of v_2 is almost zero for high $|\Delta\eta|$ bins. This might be due to the fact that softer fragmentations at low center of mass energy are dominant.

3.3.2 Effect of $|\Delta\eta|$ bins on v_2

Generally, the value of v_2 is smaller for higher $|\Delta\eta|$ bins for the same $\sqrt{s_{NN}}$ and type of particle. This can be attributed to the fact that particles from jets are more prevalent in mid-rapidity. This means that the bias is smaller for higher $|\Delta\eta|$ bins, which is reflected in a smaller value of v_2

3.3.3 Effect of quark flavor on v_2

Generally the value of ${v_2}^{\pi}(p_T) > {v_2}^{H}(p_T) > {v_2}^{\gamma^{dir}}(p_T)$. This trend is true for the low values of p_T. There is no obvious trend for higher p_T values. This may be due to the lack of statistics and of the harder fragmentation in the higher p_T bins.

3.3.4 Results Interpretation

The most notable result here is the fact that v_2 was non-zero for all the particles and for almost all the bins. Since physically we expect v_2 to be zero for all particles in PYTHIA simulations, specially for direct photons, the obvious conclusion is that those values are due to inherent biases in the way we calculate the event plane. This is further confirmed by the fact that the v_2 for direct photons is lower than v_2 for light and heavy mesons. While the bias in plane calculation happens for the near and away side for both light and heavy mesons, direct photons plane calculations would have biases in the away side only. This would explain then the lower v_2 values for the direct photons.

Given those results we can only conclude that our obtained results should be taken into account when comparing with v_2 for real experiments, by subtracting the values here from the experimental results in order to account for the event plane calculation bias.

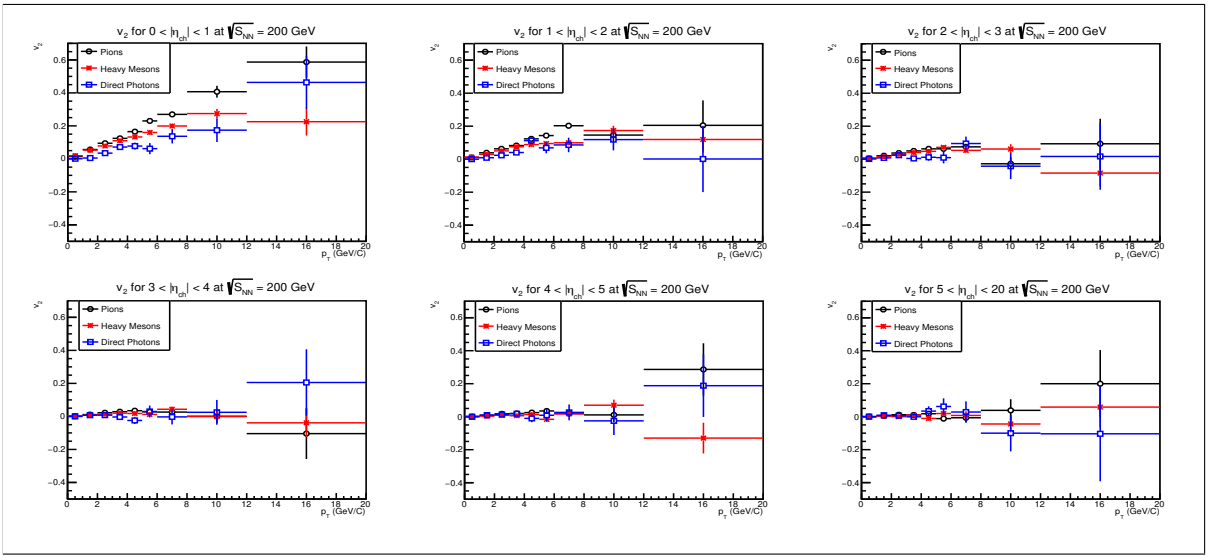

FIGURE 3.9: Elliptic flow for different pseudorapidity bins at $\sqrt{s_{nn}} = 200$ GeV

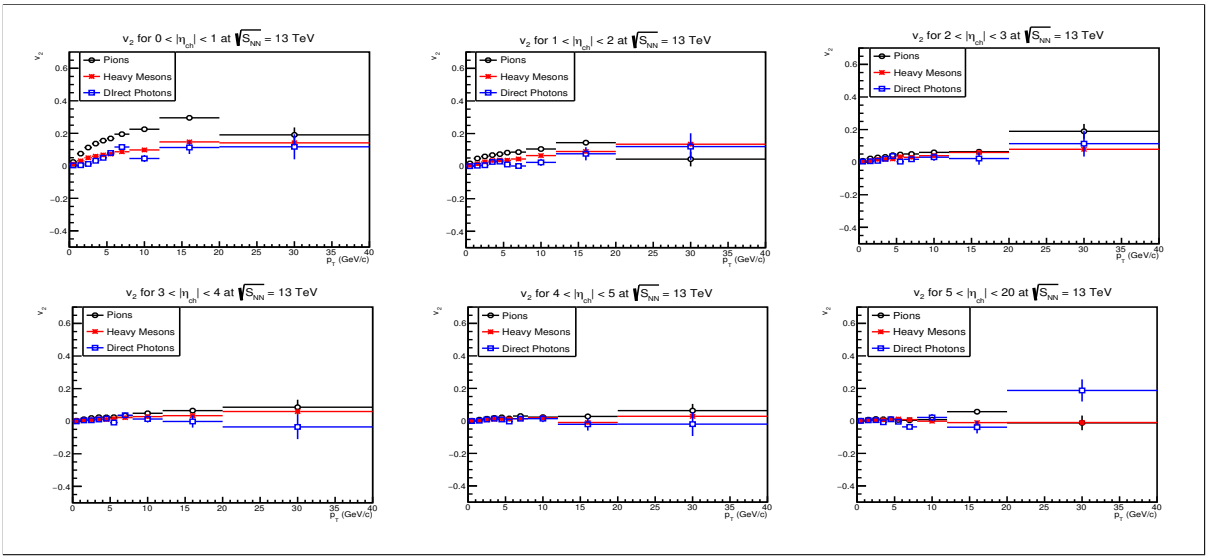

FIGURE 3.10: Elliptic flow for different pseudorapidity bins at $\sqrt{s_{nn}} = 13$ TeV

Chapter 4

Conclusion and Outlook

In the first millisecond after the Big Bang matter existed in a special state called the Quark-Gluon plasma. While in nature, quarks do not exist freely and are confined in hadrons, in this state, quarks are actually de-confined. To study matter at its most fundamental level, science is in search of ways that would allow for the replication of those conditions and the creation of this plasma in the lab. This would then allow us to study those quarks, and would mature our understanding of matter and the universe.

While deconfinment needs extreme temperatures and densities, in heavy-ion collisions, in colliders such as RHIC and LHC, the energy to which particles are accelerated are very high, well beyond the temperatures needed for phase transition into QGP, leading physicists to suspect the creation of QGP for ultra brief periods after the collisions.

Because of the brevity of time in which matter exists in this state however, any QGP would have cooled down and expanded changing to hadrons before reaching the detectors. QGP therefore can not be detected directly, but through some markers. One of the important markers used as evidence for the creation of QGP is the azimuthal anisotropy as measured by the elliptic flow. But what is the elliptic flow?

Now, a key evidence for the formation of QGP is the anisotropy in elliptic flow of produced quark-flavored particles. This suggests that the matter created right after the collision exhibits hydrodynamic behavior; in other words QGP could have been formed. [30]

But while hydrodynamic models are very successful at predicting the elliptic flow at low transverse momenta, at high momenta, the experimental measurements are higher than the predictions. The formation of QGP has been cited as a possible source for this deviation, but models with QGP still show lower levels of anisotropic flow than observed in the experiments. [31]

In this thesis then, we use PYTHIA to simulate high energy collisions and measure v_2 for the produced particles. Given that in PYTHIA there is no final state interaction, in principle v_2 should be zero for the different particles at high p_T no matter the quark flavor. Also in PYTHIA, since no medium is formed, effects of surface bias emission would not exist. Whatever values received here thus of v_2, would act as probes to be compared to the experimental measurements of v_2.

The results showed that v_2 is in general lower at the higher center of mass energy, and that as expected, ${v_2}^{\pi}(p_T) > {v_2}^{H}(p_T) > {v_2}^{\gamma^{dir}}(p_T)$. The most notable result however was the fact that v_2 was non-zero for almost all the particles and for all the bins. Since physically we expect v_2 to be zero for all particles in PYTHIA simulations, the obvious conclusion is that those values are due to inherent biases in the event plane calculation method. Those results then should be taken into account when comparing with v_2 for real experiments, by subtracting the values here from the experimental results.

Bibliography

[1] C Sutton. *standard model. Encyclopedia Britannica*. [Online; accessed 23-April-2022]. URL: https://www.britannica.com/science/Standard-Model.

[2] T. Editors of Encyclopaedia Britannica. *lepton. Encyclopedia Britannica*. [Online; accessed 23-April-2022]. URL: https://www.britannica.com/science/lepton.

[3] Kenneth S. Schmitz. "Chapter 1 - Philosophy of Science". In: *Physical Chemistry*. Ed. by Kenneth S. Schmitz. Boston: Elsevier, 2018, pp. 183–367. ISBN: 978-0-12-800513-2. DOI: https://doi.org/10.1016/B978-0-12-800513-2.00001-2. URL: https://www.sciencedirect.com/science/article/pii/B9780128005132000012.

[4] T. Editors of Encyclopaedia Britannica. *antiparticle. Encyclopedia Britannica*. [Online; accessed 30-July-2022]. URL: https://www.britannica.com/science/antiparticle.

[5] T. Editors of Encyclopaedia Britannica. *annihilation. Encyclopedia Britannica*. [Online; accessed 30-July-2022]. URL: https://www.britannica.com/science/annihilation.

[6] *Antiquark*. [Online; accessed 30-July-2022]. URL: https://www.studysmarter.us/explanations/physics/radiation/antiquark/.

[7] *The lepton family*. [Online; accessed 30-July-2022]. URL: http://hst-archive.web.cern.ch/archiv/HST2002/feynman/leptonfamily.html.

[8] *The Standard Model*.

[9] Ginés Martínez Solaeche. "Top tagging at the LHC experiments with proton-proton collisions at s = 13TeV". PhD thesis. July 2015. DOI: 10.13140/RG.2.1.4521.4560.

[10] T. Editors of Encyclopaedia Britannica. *Baryons*. [Online; accessed 30-July-2022]. URL: https://www.britannica.com/science/baryon.

[11] Gerald Feldman. "Why neutrons and protons are modified inside nuclei". In: *Nature* 556.7744 (Feb. 2019). [Online; accessed 30-July-2022], pp. 332+. URL: link.gale.com/apps/doc/A575056255/AONE?u=aucairo&sid=summon&xid=0fc414ae.

[12] T. Editors of Encyclopaedia Britannica. *meson*. [Online; accessed 30-July-2022]. URL: https://www.britannica.com/science/meson.

[13] C Sutton. *strong force. Encyclopedia Britannica*. [Online; accessed 13-May-2022]. URL: https://www.britannica.com/science/strong-force.

[14] F. Halzen and A. Martin. *Quraks and Leptons. An Introductory Course in Modern Particle Physics*. 1984.

[15] Carlos Frajuca. *As electrons are fundamental particles. Do electrons independently exist in early universe particularly in Quark Gluon Plasma (QGP)?* July 2016.

[16] André Walker-Loud. "Dissecting the Mass of the Proton". In: (). [Online; accessed 13-July-2022]. URL: https://physics.aps.org/articles/v11/118.

[17] Johann Rafelski. "Melting hadrons, boiling quarks". In: *The European Physical Journal A* 51.9 (2015). DOI: 10.1140/epja/i2015-15114-0. URL: https://doi.org/10.1140%2Fepja%2Fi2015-15114-0.

[18] Yi-Bo Yang et al. "Proton Mass Decomposition from the QCD Energy Momentum Tensor". In: *Phys. Rev. Lett.* 121 (21 2018), p. 212001. DOI: 10.1103/PhysRevLett.121.212001. URL: https://link.aps.org/doi/10.1103/PhysRevLett.121.212001.

[19] Stanislaw Mrowczynski. "Quark-Gluon Plasma". In: *arXiv* (). DOI: 10.48550/arXiv.nucl-th/9905005. eprint: https://doi.org/10.48550/arXiv.nucl-th/9905005. URL: https://doi.org/10.48550/arXiv.nucl-th/9905005.

[20] Frank Wilczek. "QCD Made Simple". In: *Physics Today* 53.8 (2000), pp. 22–28. DOI: 10.1063/1.1310117. eprint: https://doi.org/10.1063/1.1310117. URL: https://doi.org/10.1063/1.1310117.

[21] *When Matter Melts*. Accessed: 2022-07-13. June 23, 2011. URL: https://newscenter.lbl.gov/2011/06/23/when-matter-melts/.

[22] Jana N. Guenther. *Overview of the QCD phase diagram – Recent progress from the lattice*. 2020. DOI: 10.48550/ARXIV.2010.15503. URL: https://arxiv.org/abs/2010.15503.

[23] Xin An et al. "The BEST framework for the search for the QCD critical point and the chiral magnetic effect". In: *Nuclear Physics A* 1017 (2022), p. 122343. ISSN: 0375-9474. DOI: https://doi.org/10.1016/j.nuclphysa.2021.122343. URL: https://www.sciencedirect.com/science/article/pii/S0375947421002086.

[24] Joseph Favata. "Correlative Framework of Techniques for the Inspection, Evaluation, and Design of Micro-electronic Devices". In: (Jan. 2020).

[25] *Scattering Experiments and Classical Theory of AtomAtom Scattering*.

[26] R. Snellings. "Collective Expansion at the LHC: selected ALICE anisotropic flow measurements". In: *Journal of Physics G: Nuclear and Particle Physics* 41 (Aug. 2014). DOI: 10.1088/0954-3899/41/12/124007.

[27] Edmond Iancu. "QCD in heavy ion collisions". In: (2012). DOI: 10.48550/ARXIV.1205.0579. URL: https://arxiv.org/abs/1205.0579.

[28] Barbara Betz. "Jet quenching in heavy-ion collisions: The transition era from RHIC to LHC". In: *The European Physical Journal A* 48 (Nov. 2012). DOI: 10.1140/epja/i2012-12164-8.

[29] David d'Enterria. "Perturbative probes of QCD matter at the Large Hadron Collider". In: (2012). DOI: 10.48550/ARXIV.1207.4362. URL: https://arxiv.org/abs/1207.4362.

[30] Raimond Snellings. "Elliptic flow: a brief review". In: *New Journal of Physics* 13.5 (2011), p. 055008. DOI: 10.1088/1367-2630/13/5/055008. URL: https://doi.org/10.1088%2F1367-2630%2F13%2F5%2F055008.

[31] Ahmed Hamed and. "Azimuthal anisotropy (iv/isub2/sub) of high-pT sup0/supand direct in AuAu collisions at = 200 GeV". In: *Journal of Physics: Conference Series* 270 (2011), p. 012010. DOI: 10.1088/1742-6596/270/1/012010. URL: https://doi.org/10.1088/1742-6596/270/1/012010.

[32] Ahmed M. Hamed. "High-pT direct photon azimuthal correlation measurements". In: *Nuclear Physics A* 931 (2014). QUARK MATTER 2014, pp. 706–711. ISSN: 0375-9474. DOI: https://doi.org/10.1016/j.nuclphysa.2014.08.091. URL: https://www.sciencedirect.com/science/article/pii/S0375947414003510.

[33] Ahmed Hamed. "Azimuthal elliptic anisotropy (v 2) of high-pT direct in Au+Au collisions at = 200 GeV". In: *Journal of Physics: Conference Series* 589 (Mar. 2015). DOI: 10.1088/1742-6596/589/1/012009.

[34] J. Adams et al. "Experimental and theoretical challenges in the search for the quark–gluon plasma: The STAR Collaboration's critical assessment of the evidence from RHIC collisions". In: *Nuclear Physics A* 757.1-2 (2005), pp. 102–183. DOI: 10.1016/j.nuclphysa.2005.03.085. URL: https://doi.org/10.1016%2Fj.nuclphysa.2005.03.085.

[35] Chun Shen et al. "Radial and elliptic flow in Pbmml:math xmlns:mml="http://www.w3.org/1998/Math display="inline"mml:mo/mml:mo/mml:mathPb collisions at energies available at the CERN Large Hadron Collider from viscous hydrodynamics". In: *Physical Review C* 84.4 (2011). DOI: 10.1103/physrevc.84.044903. URL: https://doi.org/10.1103%2Fphysrevc.84.044903.

[36] Omar Tarek Elsherif. "Studying the QCD medium in proton-proton collisions using PYTHIA". PhD thesis. American University in Cairo, 2018.